

**Linearly Repeated Communication Systems Using
Optical Amplifiers**

by
Mangesh S. Pimpalkhare

Thesis submitted to the Faculty of the
Virginia Polytechnic Institute and State University
in partial fulfillment of the requirements for the degree of
Master of Science
in
Electrical Engineering

APPROVED:

A handwritten signature in black ink, appearing to read 'I. Jacobs', is written over a horizontal line.

Dr. I. Jacobs, Chairman

A handwritten signature in black ink, appearing to read 'Richard O. Claus', is written over a horizontal line.

Dr. R. O. Claus

A handwritten signature in black ink, appearing to read 'A. Safaai-Jazi', is written over a horizontal line.

Dr. A. Safaai-Jazi

April, 1992
Blacksburg, Virginia

C.2

LD
5455
V855
1992
P556
C.2

Linearly Repeated Communication Systems Using Optical Amplifiers

by

Mangesh S. Pimpalkhare

Dr. Ira Jacobs, Chairman

Electrical Engineering

(ABSTRACT)

Receiver sensitivity is an important parameter in the design of optical communication systems. Prior results on receiver sensitivity for on-off keying modulated direct detection systems with an optical preamplifier are generalized for the cases of frequency-shift keying and subcarrier modulation. Our results, obtained by using the Gaussian approximation, are compared to those obtained by an 'exact' analysis. The results are also generalized for N-ary modulation schemes and systems having optical amplifiers as linear repeaters.

Simple analytic formulae are derived for the maximum system gain of optical amplifiers systems for the following two cases : 1) Constant signal power at each amplifier. 2) Equal amplifier spacing, which ensures constant total power at each amplifier. The functional dependence of system gain on various system parameters, and the effects of optical filtering at the receiver as well as at the intermediate amplifiers, is studied. The analysis is extended to include the effects of random power variations at the output of each amplifier.

Acknowledgements

I am indebted to my advisor Dr. Ira Jacobs for his ceaseless encouragement and guidance during the course of this thesis. The numerous stimulating discussions I have had with him and the knowledge and insight that I have gained from them have been the most rewarding experiences during my graduate study.

I would like to thank Dr. A. Safaai-Jazi and Dr. R. O. Claus for being on my advisory committee.

I sincerely appreciate the help provided by Dr. Ashish Vengsarkar, Mike Gunther, Russ May and Kent Murphy at various points of my work. I would also like to thank my friends, in particular my wife, for their continuous support, encouragement and help.

Last but not the least, I would like to thank AT&T Bell Laboratories for sponsoring this work and FEORC for the material support provided.

Table of Contents

1.0	Introduction	1
1.1	Receiver Sensitivity	2
1.2	Maximum System Gain	3
2.0	Receiver Sensitivity	5
2.1	Receiver Sensitivity For Binary FSK System	7
2.2	Binary Subcarrier Modulation (IM/PRK)	12
2.3	Comparison With 'Exact' Receiver Sensitivity	15
2.4	N-ary Modulation Schemes	18
2.5	Hybrid Systems	20
2.6	Discussion	21
3.0	Maximum System Gain	23
3.1	Optical Signal To Noise Ratio	24
3.2	Analysis For Maximum System Gain	26
3.3	Examples	34
3.4	Computer Simulation For Soft Gain Saturation Model	38
3.5	Effect Of Output Power Variations	41
3.6	Discussion	46
4.0	Conclusions	49

References77

Vita80

List of Illustrations

Figure 1.	Receiver model for binary FSK system	53
Figure 2.	Receiver sensitivity for binary FSK for different values of amplifier gain	54
Figure 3.	Comparison of receiver sensitivity for binary FSK and OOK for large values of amplifier gain	55
Figure 4.	Receiver model for binary subcarrier modulation system	56
Figure 5 (a).	Noise power due to $x^2(t)$, $y^2(t)$	57
Figure 5 (b).	Noise power due to $n(t)$	57
Figure 5 (c).	Noise power due to $2A[1+m\cos(w_s t)]^{1/2}x(t)$	57
Figure 6.	Comparison of receiver sensitivity obtained using Gaussian approximation with 'exact' receiver sensitivity [4], with $k=6$	58
Figure 7.	Comparison of receiver sensitivity obtained using Gaussian approximation with 'exact' receiver sensitivity [4], with $k'=$ 5.85 (using correction factor)	59
Figure 8.	Comparison of receiver sensitivity obtained using Gaussian approximation with 'exact' receiver sensitivity [4] for FSK, with $k=6$	60
Figure 9.	Comparison of receiver sensitivity obtained using Gaussian approximation with 'exact' receiver sensitivity [4] for FSK, with $k'=5.65$ (using correction factor)	61
Figure 10.	Receiver model for N-ary FSK system	62
Figure 11.	Optical amplifier model	63
Figure 12.	Effect of gain saturation in reducing maximum achievable system gain (Case I)	64

Figure 13.	Effect of gain saturation in reducing maximum achievable system gain (Case I)	65
Figure 14.	Effect of gain saturation in reducing maximum achievable system gain (Case II)	66
Figure 15.	Effect of gain saturation in reducing maximum achievable system gain (Case II)	67
Figure 16.	System gain as a function of amplifier gain, for Cases I and II	68
Figure 17.	System gain as a function of number of amplifiers used, for Cases I and II	69
Figure 18.	Effect of optical filtering on system gain, for Case I	70
Figure 19.	Effect of optical filtering on system gain, for Case II	71
Figure 20.	System gain as a function of power transmitted, for Case II	72
Figure 21.	Propagation of signal and noise in a chain of identical, equally spaced amplifiers	73
Figure 22.	Saturated amplifier gains in a chain of identical, equally spaced amplifiers	74
Figure 23.	Comparison of system gain obtained by analytic formulae and by computer simulation	75
Figure 24.	Effect of output power variations in reducing system gain	76

List of Tables

Table 1. List of Symbols used51

1.0 Introduction

Optical amplifier technology has been instrumental in the realization of all-optical communication systems, both for high speed long-haul networks, as well as other applications. Optical amplifiers are devices which can increase the amplitude of the optical signal substantially [1], while adding very small amounts of noise. These devices can be used as preamplifiers, booster amplifiers, or as linear repeaters in optical communication systems. Besides getting rid of electronic regenerators, optical amplifier based systems have the added advantage of being transparent to the signal bit rate and modulation format. The use of optical amplifiers also allows the continued use of simple direct detection receivers in high capacity, long-haul communication systems. Such systems can also support wavelength division multiplexing (WDM) technology, which is effective in exploiting the tremendous transmission bandwidth of low loss fibers. Optical amplifier technology has the potential of significantly improving upon the performance of previous

generation fiber optic systems [2], in terms of capacity as well as transmission distance without electronic regeneration, while reducing the cost as well as complexity of such communication systems and networks.

Although optical amplifiers can be of several types, most current interest is in laser amplifiers, particularly erbium doped fiber amplifiers (EDFAs). The term optical amplifier is used henceforth in this thesis synonymously with an EDFA, unless indicated otherwise. Given their tremendous scope for practical applications, there is considerable interest in understanding the fundamental and practical limitations of communication systems using optical amplifiers. There has been considerable research in modeling the behavior of optical amplifiers, as well as evaluating the communication performance of systems using optical amplifiers. This thesis focuses on some aspects of the communication performance and limitations of systems using optical amplifiers. The emphasis is on how amplifier parameters like gain, bandwidth, noise and linearity, affect system performance. The two specific problems addressed are those of finding analytic results for the receiver sensitivity and for the maximum system gain of optical amplifier systems. The following two Sections 1.1 and 1.2 give an introduction to these problems, which are analyzed in detail in Chapters 2 and 3 respectively.

1.1 Receiver Sensitivity

Receiver sensitivity is an important quantity for any communication system, since it gives the minimum signal power required at the receiver to achieve a given system performance (which is specified in terms of bit error rate for digital systems and in terms of signal to noise ratio for analog systems). Chapter 2 focuses on the problem of finding the

receiver sensitivity for optical communication systems using optical amplifiers as a preamplifier as well as linear intermediate repeaters, and employing a direct detection receiver. The Gaussian approximation, in which the noise at the receiver is assumed to have a Gaussian probability distribution, is often used in order to simplify the analysis of the receiver sensitivity problem [3]. The methodology for finding the receiver sensitivity of a direct detection receiver with an optical preamplifier, using the Gaussian approximation, is discussed in Chapter 2. Results are given for the cases of on-off keying (OOK) modulation, frequency shift keying (FSK) modulation and subcarrier modulation. The dependence of receiver sensitivity on system parameters is also discussed.

There have been several recent papers on the subject of “exact” receiver sensitivity of direct detection fiber optic systems using optical amplifiers. Some of our results, which are obtained using the Gaussian approximation, are compared with those obtained by an ‘exact’ analysis in [4]. The extension of the results for receiver sensitivity to systems having N-ary modulation formats and to hybrid systems having optical amplifiers as linear repeaters, is also summarized in Chapter 2.

1.2 Maximum System Gain

For fiber optic systems using optical amplifiers, it is of interest to determine the maximum system gain (which is the reciprocal of the system loss), since this quantity determines the maximum span of the system without electronic regeneration for a given system performance. Systems using optical amplifiers are limited in terms of the distance they can span mainly because of the build up of amplified spontaneous emission (ASE) noise [1], [5] generated in each amplifier. The accumulation of ASE noise depends on

optical amplifier parameters, as well as on factors such as optical filtering. Chapter 3 presents an analysis which models the propagation of signal and noise in a system having a chain of optical amplifiers. Analytical results are obtained for the maximum system gain of such systems. The dependence of system gain on various system parameters and the trade-off involved in minimizing the system gain are also discussed. These analytical results are derived on the basis of a simplified amplifier model. The results are validated by a computer simulation performed for a more realistic amplifier model [5]. The effect of random variations in the total power at the output of each amplifier in a chain of optical amplifiers, is also discussed in Chapter 3.

Chapter 4 summarizes the important results and conclusions of this thesis, and gives a perspective on the scope for future work.

2.0 Receiver Sensitivity

For digital communication systems, receiver sensitivity is defined as the minimum signal power required at the receiver to achieve a given signaling rate and bit error rate (BER). This signal power can be expressed in Watts, dBm, or for optical systems in terms of the equivalent number of photons/bit [1], [6]. The advantage of expressing the receiver sensitivity in photons/bit is that the sensitivity in photons/bit N_p is also the normalized signal to noise ratio, analogous to the energy-per-bit to noise-per-unit-bandwidth ratio E/N , which is used in the calculation of BER of communication systems [7]. Also, there is a theoretical minimum for N_p , which facilitates comparing the performance of an actual receiver with the theoretical ideal.

The problem of evaluating the receiver sensitivity for systems with optical preamplifiers has been addressed in several papers [2], [3], [4], [8], [9], [10]. Most of these prior results related to receiver sensitivity have been obtained for an on-off keying

(OOK) modulation format, although there has been recent work which includes results for other modulation formats [4]. We generalize some prior results in [11], to derive an explicit formula for the receiver sensitivity of a direct detection system with an optical preamplifier and a binary frequency shift keying (FSK) modulation format. The methodology followed here is the same as that in [3], [11], which uses the Gaussian approximation to the noise statistics at the receiver.

Another modulation format that is of interest, especially in multiuser communications, is subcarrier modulation [12]. We derive analytical results for the receiver sensitivity of a direct detection system with an optical preamplifiers and a subcarrier modulation format, using a Gaussian approximation for the noise at the subcarrier demodulation circuit.

The validity and accuracy of the receiver sensitivity obtained using the Gaussian approximation has been discussed in some recent papers [4], [9]. We compare some of our results with those obtained by an ‘exact’ analysis in [4]. It is shown how the results obtained by the approximate analysis can be made to be close to those obtained by ‘exact’ analyses by using simple scale factor corrections.

One of the ways to improve the receiver sensitivity is to increase the signal alphabet size [13]. We discuss the methodology for evaluating the receiver sensitivity for N-ary FSK and N-ary subcarrier modulation. We also show how all the results obtained for the receiver sensitivity of a system having a preamplifier can be generalized to systems with optical amplifiers as linear intermediate repeaters.

2.1 Receiver Sensitivity For Binary FSK System

For an OOK communication system using an optical preamplifier, the receiver sensitivity is given [11] by (refer to Table 1 for definition of all symbols used in Chapter 2)

$$N_p = 36n_{sp} \frac{(G-1)}{G} \left[1 + \frac{1}{6} \sqrt{BT + \left[\frac{N_1}{6n_{sp}(G-1)} \right]^2} \right] \quad (2.1.1)$$

where N_p is the average number of photons required at the receiver to achieve a BER of 10^{-9} . In (2.1.1), G is the amplifier gain, B is the optical bandwidth, T is the bit period, and $n_{sp} \geq 1$ is the spontaneous emission factor. N_1 is the receiver sensitivity in the absence of an optical preamplifier and is typically several thousand photons/bit for a good PIN detector followed by a low-noise electronic amplifier [11] (The term in the square brackets with N_1 as the numerator accounts for the thermal noise at the receiver). This formula is derived assuming that there is a polarization filter at the receiver, which filters out the optical noise in one of the two orthogonal polarization modes of the fiber. Under this assumption, the optical noise has a noise spectral density of $n_{sp}(G-1)hf$ at the output of the receiver preamplifier. This implies that the noise spectral density referred to the preamplifier input is $n_{sp}(1-1/G)hf$ [3]. The results obtained in this Chapter are consistent with these assumptions. The results can be easily generalized, as done in Chapter 3, for the case where there is no polarization filter at the receiver, by simply replacing n_{sp} by $2n_{sp}$ in all the formulae for receiver sensitivity.

In the case of binary FSK, there are two orthogonal signals, each at a different center frequency. It is assumed that a '1' is transmitted using a rectangular pulse whose center frequency is f_1 and a '0' is transmitted using a rectangular pulse whose center frequency is f_2 . In addition, it is assumed that each of the two frequency channels have the same average received power P_r .

Figure 1 shows a direct detection receiver for a binary FSK modulation format. There are two bandpass optical filters, each of bandwidth B and centered about frequencies f_1 and f_2 respectively, followed by photodetectors (one for each frequency channel) and integrating circuits (one for each channel), which act as low pass filters [9]. A decision is made that a '1' was transmitted if the difference between currents I_1 and I_2 exceeds a threshold value I_{th} . The optimal threshold I_{th} and the resulting probability of error, are obtained in the analysis in this section.

It is assumed that the electrical amplifier is an ideal integrator that measures the total energy in the pulse and that the integral can be approximated by a sum, where the sampling time is given by $1/B$, so that there are $m = BT \gg 1$ samples [6]. With these assumptions, the currents I_1 and I_2 when a '1' is transmitted, are given by

$$I_1 = \frac{1}{B} \sum_{i=1}^{BT} [(A+x_i)^2 + y_i^2] + n \quad (2.1.2)$$

$$I_2 = \frac{1}{B} \sum_{i=1}^{BT} [x_i^2 + y_i^2] + n \quad (2.1.3)$$

In (2.1.2) and (2.1.3), x_i and y_i are respectively the samples of the inphase and quadrature phase components of the optical noise, while n is the thermal noise. Similarly, when a "0" is transmitted, I_1 and I_2 are given by

$$I_1 = \frac{1}{B} \sum_{i=1}^{BT} [x_i^2 + y_i^2] + n \quad (2.1.4)$$

$$I_2 = \frac{1}{B} \sum_{i=1}^{BT} [(A+x_i)^2 + y_i^2] + n \quad (2.1.5)$$

Let $I = I_1 - I_2$. It is assumed that I_1 and I_2 are Gaussian distributed [3], which enables the moments of I to be easily calculated. When a '1' is transmitted, it can be seen from (2.1.2)

and (2.1.3) that the moments of I are given by

$$\mu_1 = \frac{1}{B}[A^2m] = A^2T \quad (2.1.6)$$

$$\sigma_1^2 = \frac{T}{B}[4A^2\sigma_{oa}^2 + 8\sigma_{oa}^4] + 2\sigma_n^2 \quad (2.1.7)$$

When a “0” is transmitted, the moments of I can be obtained from (2.1.4) and (2.1.5) and are given by

$$\mu_0 = -\frac{1}{B}[A^2m] = -A^2T \quad (2.1.8)$$

$$\sigma_0^2 = \frac{T}{B}[4A^2\sigma_{oa}^2 + 8\sigma_{oa}^4] + 2\sigma_n^2 \quad (2.1.9)$$

If the decision threshold I_{th} is set such that both types of errors are equally likely, then it is easily shown that

$$I_{th} = \frac{\sigma_0\mu_1 + \sigma_1\mu_0}{\sigma_0 + \sigma_1} \quad (2.1.10)$$

and probability of error is given by

$$P_e = Q\left[\frac{\mu_1 - \mu_0}{\sigma_1 + \sigma_0}\right] \quad (2.1.11)$$

Using (2.1.6) - (2.1.9) in (2.1.10), it can be seen that $I_{th} = 0$. Using (2.1.6) - (2.1.9) in (2.1.11), we get

$$P_e = Q\left[\frac{A^2T}{\sqrt{\frac{T}{B}(4A^2\sigma_{oa}^2 + 8\sigma_{oa}^4) + 2\sigma_n^2}}\right] \quad (2.1.12)$$

Here $Q(k)$ is the area under the Gaussian tail, as defined in Table 1. For an error probability of 10^{-9} , $k = 6$. Setting the quantity in the square brackets in (2.1.12) equal to 6 gives

$$A^2T = 6 \sqrt{\frac{T}{B}(4A^2\sigma_{oa}^2 + 8\sigma_{oa}^4) + 2\sigma_n^2} \quad (2.1.13)$$

The signal amplitude A is related to the receiver sensitivity in photons/bit

N_p by

$$A^2T = (P_r G/R_b)(q\eta/hf) = N_p G q\eta \quad (2.1.14)$$

(2.1.14) is obtained assuming an ideal photodetector with responsivity ($q\eta/hf$). As mentioned before, the optical noise at the amplifier input is assumed to be white Gaussian with a one-sided spectral density of $n_{sp}(1-1/G)hf$ [3]. It follows that the variance of the inphase and quadrature components of the optical noise, x_i and y_i , is given by

$$\sigma_{oa}^2 = \frac{1}{2} n_{sp}(G-1)Bq\eta \quad (2.1.15)$$

The variance of the thermal noise component n is given by

$$\sigma_n^2 = \frac{2\kappa(290)}{ZR_b} \quad (2.1.16)$$

In (2.1.16), κ is Boltzmann's constant, not to be confused with the k defined in Table 1, and Z is the effective noise impedance of the electrical receiver. Using (2.1.14) - (2.1.16) in (2.1.13) gives an expression for the receiver sensitivity as

$$N_p = 36n_{sp} \frac{(G-1)}{G} \left[1 + \frac{1}{3} \sqrt{9 + \frac{1}{2}BT + \frac{\kappa(290)}{ZR_b [n_{sp}(G-1)q\eta]^2}} \right] \quad (2.1.17)$$

As $G \rightarrow 1$, $N_p \rightarrow N_1$. From (2.1.17), we get

$$N_1 = \sqrt{\frac{144\kappa(290)}{ZR_b(q\eta)^2}} \approx 4200 \text{ photons/bit} \quad (2.1.18)$$

The noise impedance is inversely proportional to R_b (this corresponds to a constant effective noise capacitance, see [11]). Using typical values [11], $N_1 \approx 4200$ photons/bit. N_1 is the receiver sensitivity in the thermal noise limit (no optical preamplifier). Using (2.1.18) in (2.1.17) we get the expression for the receiver sensitivity as

$$N_p = 36n_{sp} \frac{(G-1)}{G} \left[1 + \frac{1}{3} \sqrt{9 + \frac{1}{2}BT + \left[\frac{N_1}{12n_{sp}(G-1)} \right]^2} \right] \quad (2.1.19)$$

(2.1.19) gives the receiver sensitivity as a function of various system parameters. Figure 2 shows a plot of N_p as a function of BT , for various values of amplifier gain G . It can be seen that for $G > 25$ dB, the sensitivity is approximately equal to that obtained as $G \rightarrow \infty$, which is

$$N_\infty = 36n_{sp} \left[1 + \frac{1}{3} \sqrt{9 + \frac{1}{2}BT} \right] \quad (2.1.20)$$

It can be seen from (2.1.1) that the receiver sensitivity in the limit of large gain, for OOK is

$$N_\infty = 36n_{sp} \left[1 + \frac{1}{6} \sqrt{BT} \right] \quad (2.1.21)$$

It follows from (2.1.20) and (2.1.21) that for large amplifier gains, the effect of thermal noise becomes negligible. For $n_{sp} = 1$, $BT = 1$, (2.1.20) gives a receiver sensitivity of 73 photons/bit for binary FSK, as compared to a sensitivity of 42 photons/bit given by (2.1.21) for OOK. This suggests that binary FSK gives a significantly poorer performance compared to OOK. However, an 'exact' analysis [4] for receiver sensitivity shows that binary FSK is only slightly poorer (40 photons/bit as compared to 38 photons/bit for OOK) than OOK at $BT = 1$. This discrepancy is due to the fact that the Gaussian approximation used in our analysis is not very accurate for small values of BT . However, for large BT , the Gaussian approximation is expected to give better results. From (2.1.20) and (2.1.21), it can be seen that for large BT , the receiver sensitivity for binary FSK is about 2 dB poorer than the sensitivity for OOK (For $BT \gg 1$ and $n_{sp} = 1$, the receiver sensitivity for binary FSK is approximately equal to $8.5\sqrt{BT}$, as opposed to $6\sqrt{BT}$ for OOK). Figure 3 shows the receiver sensitivity as a function of BT , in the limit of large amplifier gain, for OOK and binary FSK.

2.2 Binary Subcarrier Modulation (IM/PRK)

For a subcarrier modulation format, the optical carrier wave is intensity modulated by an electrical subcarrier, which is modulated by the information source signal, using a scheme such as phase shift keying (PSK). We consider here the problem of finding the receiver sensitivity for a binary intensity modulation (IM) format, where the subcarrier is modulated using phase reversal keying (PRK). For such an IM/PRK system, a '1' corresponds to a received optical power given by $P_0[1+m \cos(\omega_s t)]$, where P_0 is the peak power, m is the subcarrier modulation index and ω_s is the subcarrier frequency. The '0' corresponds to a received power given by $P_0[1-m \cos(\omega_s t)]$.

The direct detection receiver for this modulation format is shown in Figure 4. The receiver has an optical preamplifier of bandwidth B , followed by a photodetector, followed by an electrical bandpass filter of bandwidth B_e . Assuming that the noise present at the output of the electrical bandpass filter is narrowband Gaussian distributed, the bit error probability can be estimated in terms of the normalized signal to noise ratio E/N (ratio of the energy per bit to noise power spectral density) at the input of the subcarrier demodulation circuit. The receiver sensitivity can then be found for a specified bit error probability.

The first step is to calculate the signal power and the total noise power at the output of the electrical bandpass filter. The output of the photodetector, after addition of electrical thermal noise is given by

$$I = \left\{ A\sqrt{1+m \cos(\omega_s t)} + x(t) \right\}^2 + y^2(t) + n(t) \quad (2.2.1)$$

Here $x(t)$ and $y(t)$ are respectively the inphase and quadrature components of the optical noise, and $n(t)$ is the thermal noise. The signal power is due to the two terms A^2 and $A^2 m \cos(\omega_s t)$, while the noise power is due to the four terms $x^2(t)$, $y^2(t)$, $n(t)$ and $2A[1+m \cos(\omega_s t)]^{1/2}x(t)$. The signal I is passed through an electrical bandpass filter of bandwidth

B_e . It is assumed that the noise power spectral density at the output of the filter is the sum of the power spectral densities of each of the four noise terms. Figure 5(a) shows the power spectral density of $x(t)$, $y(t)$ and $x^2(t)$, $y^2(t)$. The spectral density of $x^2(t)$ and $y^2(t)$ has a triangular shape, as shown in Figure 5 (a), where the spectral density $P_2(f)$ is given by

$$P_2(f) = \left[\frac{1}{2} n_{sp}(G-1)q\eta \right]^2 f + \left[\frac{1}{2} n_{sp}(G-1)q\eta \right]^2 B \quad (2.2.2)$$

for $0 \leq f \leq B$. The noise power due to $x^2(t)$ (and $y^2(t)$) is obtained by putting $f = f_s$ in (2.2.2) and multiplying the resulting right hand side by $2B_e$ (See Figure 5 (a)). It follows that the equivalent Gaussian distributed noise due to $x^2(t)$ and $y^2(t)$, after bandpass filtering, has a power given by

$$N_{sp-sp} = [n_{sp}(G-1)q\eta]^2 (B-f_s) B_e \quad (2.2.3)$$

where N_{sp-sp} is termed the “spontaneous-spontaneous beat noise”. Figure 5(b) shows the power spectral density of the thermal noise term $n(t)$. It follows that the equivalent Gaussian distributed noise due to $n(t)$, after bandpass filtering, has a power given by

$$N_{th} = B_e \frac{4k(290)}{Z} = 2 \frac{B_e}{T} \sigma_n^2 \quad (2.2.4)$$

We assume that the terms $2Ax(t)$ and $[1+m \cos(\omega_s t)]^{1/2}$ are independent and jointly stationary. Consequently, the power spectral density of $2A[1+m \cos(\omega_s t)]^{1/2}x(t)$ is given by the convolution of the power spectral density of $2Ax(t)$ and the power spectral density of $[1+m \cos(\omega_s t)]^{1/2}$ [7], which is shown in Figure 5(c). It can be shown that the equivalent Gaussian distributed noise due to $2A[1+m \cos(\omega_s t)]^{1/2}x(t)$, after bandpass filtering, has a power given by

$$N_{s-sp} = 2\left(2 + \frac{m^2}{2}\right) A^2 B_e [n_{sp}(G-1)q\eta] \quad (2.2.5)$$

N_{s-sp} is termed the “signal-spontaneous beat noise”. The total equivalent noise power at

the input of the subcarrier demodulation circuit is given by

$$N = N_{sp-sp} + N_{th} + N_{s-sp} \quad (2.2.6)$$

where N_{sp-sp} , N_{th} , and N_{s-sp} are given by (2.2.3), (2.2.4) and (2.2.5) respectively. The signal power at the input of the demodulation circuit, due to A^2 and $A^2m \cos(\omega_s t)$, after bandpass filtering is given by

$$S = \frac{A^4 m^2}{2} \quad (2.2.7)$$

From (2.2.7) and (2.2.6), it follows that the normalized electrical signal to noise ratio E/N at the input of the subcarrier demodulation circuit is given by

$$\frac{E}{N} = \frac{A^4 m^2 T^2}{2 [n_{sp}(G-1)q\eta]^2 (B-f_s)T + 4\sigma_n^2 + 4\left(2 + \frac{m^2}{2}\right)A^2 T [n_{sp}(G-1)q\eta]} \quad (2.2.8)$$

Assuming that the subcarrier demodulation is done synchronously (coherent detection), the error probability is given in terms of the normalized signal to noise ratio [7] by

$$P_e = Q\left(\sqrt{2\frac{E}{N}}\right) \quad (2.2.9)$$

It can be seen from (2.2.9) that for $P_e = 10^{-9}$, $E/N = 18$. From (2.2.8), we get

$$A^4 m^2 T^2 = 18 \left\{ 2 [n_{sp}(G-1)q\eta]^2 (B-f_s)T + 4\sigma_n^2 + 4\left(2 + \frac{m^2}{2}\right)A^2 T [n_{sp}(G-1)q\eta] \right\} \quad (2.2.10)$$

The signal amplitude A is related to the photons/bit at the receiver N_p by

$$\frac{A^2}{R_b} = N_p G q \eta \quad (2.2.11)$$

It follows from (2.2.10) and (2.2.11) that the receiver sensitivity at $P_e = 10^{-9}$ is given by

$$N_p = \frac{18(m^2+4)}{m^2} n_{sp} \frac{(G-1)}{G} \left[1 + \frac{m^2}{18(m^2+4)} \sqrt{\left[\frac{18(m^2+4)}{m^2} \right]^2 + \frac{36(B-f_s)T}{m^2} + \frac{N_1}{[n_{sp}(G-1)]^2}} \right] \quad (2.2.12)$$

where N_1 is the receiver sensitivity as $G \rightarrow 1$, and is given by (2.1.18). It can be seen from (2.2.12) that the expression for receiver sensitivity for subcarrier modulation has the same functional form as in the case of on-off keying and frequency shift keying. However, the receiver sensitivity for the case of subcarrier modulation is considerably poorer compared to that for OOK or FSK. For example, if the amplifier gain is assumed large and the thermal noise is neglected, (2.2.12) gives a sensitivity of 180 photons/bit for $m=1$, $BT=1$, $n_{sp}=1$. In practice, the receiver sensitivity for a subcarrier modulated system will be much poorer than 180 photons/bit, since BT is usually large compared to 1. For $m = 1$ and large values of amplifier gain G , the receiver sensitivity given by (2.2.12) simplifies to

$$90n_{sp} \left[1 + \frac{1}{90} \sqrt{8100 + 36BT} \right] \quad (2.2.13)$$

It follows from (2.2.13) that for $BT \gg 1$ and $m = 1$, the receiver sensitivity for subcarrier modulation is approximately given by $6\sqrt{BT}$, which is same as the approximate receiver sensitivity for OOK for $BT \gg 1$. However, for subcarrier modulation m is generally restricted to values much smaller than unity to achieve appropriate linearity. For $m < 1$, the receiver sensitivity for subcarrier modulation would be poorer compared to that for OOK, even for large values of BT .

2.3 Comparison With ‘Exact’ Receiver Sensitivity

The analysis in the previous sections is based on the Gaussian approximation to the noise statistics at the input to the decision circuit. There have been several recent papers [4], [9], which address the validity and accuracy of using such an approximation in the derivation of receiver sensitivity. We compare some of our results with the ‘exact’ results

obtained in [4]. In this ‘exact’ analysis, the ASE noise is considered to be the dominant noise source. For OOK, (2.1.1) and (2.1.21) can be generalized to give the receiver sensitivity at any probability of error $P_e = Q(k)$. When thermal noise is neglected, and the gain of the optical amplifier is assumed to be sufficiently large, (so that $(G-1) \approx G$), the receiver sensitivity to achieve $P_e = Q(k)$ is given by

$$N_{\infty} = k^2 n_{sp} \left[1 + \frac{1}{k} \sqrt{BT} \right] \quad (2.3.1)$$

Figure 6 compares the receiver sensitivity given by (2.3.1) with $k = 6$ (for a $P_e = 10^{-9}$), with the ‘exact’ receiver sensitivity for $P_e = 10^{-9}$, using the results obtained in [4]. It can be seen that the Gaussian approximation leads to a poorer receiver sensitivity for a given probability of error. The receiver sensitivity predicted by the Gaussian approximation is about 0.4 dB poorer than the ‘exact’ receiver sensitivity at $BT = 1$. For large values of BT , the approximate receiver sensitivity is poorer by about 0.2 dB.

The results obtained by using the Gaussian approximation can be made to match more closely with the ‘exact’ results by using simple scale factor corrections. If we use k' instead of k in (2.3.1), where $k' = (k + \text{correction factor})$, the receiver sensitivity given by (2.3.1) can be made to be close to that given by the ‘exact’ results for a $P_e = Q(k)$, with a proper choice of the correction factor. For example, for $P_e = 10^{-9}$, $k = 6$ since $Q(6) = 10^{-9}$. Instead of using $k = 6$ in (2.3.1), if we use $k' = 5.85$, the receiver sensitivity given by (2.3.1) closely matches with the corresponding ‘exact’ receiver sensitivity. This is shown in Figure 7. It should be noted that the correction factor as defined above is always negative for any P_e , since the ‘exact’ receiver sensitivity is always better than the corresponding receiver sensitivity obtained using the Gaussian approximation.

For binary FSK, the approximate receiver sensitivity to achieve $P_e = Q(k)$ is given by (generalizing (2.1.20) for any $P_e = Q(k)$)

$$N_{\infty} = k^2 n_{sp} \left[1 + \frac{1}{k} \sqrt{k^2 + 2BT} \right] \quad (2.3.2)$$

Figure 8 shows a comparison of the approximate receiver sensitivity for binary FSK, given by (2.3.2) with $k = 6$ (for $P_e = 10^{-9}$), with the corresponding 'exact' receiver sensitivity for $P_e = 10^{-9}$. It can be seen that similar to the OOK case, the Gaussian approximation predicts a poorer receiver sensitivity compared to the 'exact' receiver sensitivity. At $BT = 1$, the approximate sensitivity is poorer by 2.6 dB, and for large values of BT the approximate sensitivity is poorer by about 0.4 dB, compared to the 'exact' values. As discussed before, we can use simple scale factor corrections to give more realistic results, while still using the simple formulae derived using the Gaussian approximation. Figure 9 shows a comparison of the receiver sensitivity given by (2.3.2) with $k' = 5.65$ instead of $k = 6$, with the 'exact' sensitivity for $P_e = 10^{-9}$.

It has been shown that the use of simple empirical scale factor corrections can give fairly accurate results even with simple, approximate formulae for receiver sensitivity. It should also be noted that receiver sensitivity calculations usually make several simplifying assumptions, which do not correspond precisely to practical systems. Hence, for practical systems, the conservative estimates of receiver sensitivity given by the Gaussian approximation may be more realistic than the 'exact' results. Although the Gaussian approximation gives reasonably good results for receiver sensitivity, it should be noted that it may not give good results for where the threshold should be set [4].

2.4 N-ary Modulation Schemes

The receiver sensitivity in photons/bit of an optical communication system with an optical preamplifier is the ratio of the optical energy per bit to the photon energy, which is analogous to the energy-per-bit to the noise-per unit-bandwidth E/N ratio used in the BER calculations of communication systems [4]. This ratio is a measure of the power efficiency of the system. It is known that this receiver sensitivity can be improved for an incoherent or direct detection communication system as the signal alphabet N becomes large (for binary signaling, $N = 2$) [13]. Hence, it is of interest to determine the receiver sensitivity for N-ary modulation schemes. The analysis in the preceding sections can be extended to give the approximate receiver sensitivity for N-ary FSK and N-ary subcarrier (IM/N-ary PSK) modulation.

For N-ary FSK, the signal can occur in any one of N nonoverlapping frequency bands, centered at f_i , $i = 1, 2, \dots, N$. The receiver consists of N bandpass filters, each of bandwidth B , centered at the respective frequencies f_i . The filter outputs are passed through photodetectors and electrical integrators, as shown in Figure 10. A decision is made that the i^{th} signal was transmitted if the corresponding current I_i at the output of the respective integrator is larger than any of the other $(N-1)$ output currents.

Although an explicit expression can be found for the symbol error probability in this case [13], it is simpler to find a union upper bound on the symbol error probability, which is given by [14]

$$P_s \leq (N-1)P_e = (N-1) Q\left(\frac{\mu_1 - \mu_0}{\sigma_1 + \sigma_0}\right) \quad (2.4.1)$$

Here P_s is the symbol error probability and P_e is the bit error probability for binary FSK. Since $Q(k)$ is a steep function of k (a small change in the value of k causes a large change in

the value of $Q(k)$, we can get a reasonable (though conservative) estimate for the ratio $(\mu_1 - \mu_2)/(\sigma_1 + \sigma_2)$, by setting

$$P_s \approx (N-1) Q\left(\frac{\mu_1 - \mu_0}{\sigma_1 + \sigma_0}\right) \quad (2.4.2)$$

The upper bound on the bit error probability is the same as that on the symbol error probability [7]. Consequently, we get

$$P_e \approx (N-1) Q\left(\frac{\mu_1 - \mu_0}{\sigma_1 + \sigma_0}\right) = Q(k) \quad (2.4.3)$$

For a specified P_e and N , we can get the value of k from (2.4.3). For example, for $P_e = 10^{-9}$ and $N = 16$, $k = 6.5$ (as opposed to $k = 6$ for binary FSK). For N -ary FSK, which has N signals of equal average power, the signal amplitude is now related to the receiver sensitivity N_p in photons/bit by

$$A^2 T = (P_r G / R_b) (q \eta / h f) = N_p \log_2 N G q \eta \quad (2.4.4)$$

since there are $\log_2 N$ bits of information that can be sent per N -ary symbol. Following a similar methodology as that for finding the receiver sensitivity for binary FSK, it can be shown that the receiver sensitivity in photons/bit for N -ary FSK, to achieve a BER of $Q(k)$ is given by

$$N_p = \frac{k^2 n_{sp} (G-1)}{\log_2 N G} \left[1 + \frac{1}{k} \sqrt{k^2 + 2BT + \left[\frac{N_1 \log_2 N}{k n_{sp} (G-1)} \right]^2} \right] \quad (2.4.5)$$

It can be seen that for $N=2$ (binary FSK), (2.4.5) is the same as (2.1.19), which gives the receiver sensitivity for binary FSK. It should be noted that in (2.4.5), T is the symbol period, which is the reciprocal of the signaling rate in N -ary symbols/sec. For example, consider $N = 16$ and $BT = 1$, $n_{sp} = 1$. If the thermal noise is neglected and the gain is assumed large, (2.4.5) gives a receiver sensitivity of 19 photons/bit (using $k = 6.5$), as compared to a sensitivity of 73 photons/bit for binary ($N = 2$) FSK with the same

parameters. Thus, increasing the signal alphabet size improves the receiver sensitivity, albeit at the cost of making the receiver more complex.

In the case of N-ary subcarrier modulation, the N signals correspond to a receiver power given by $P_0[1+m \cos(\omega_s t + 2\pi i/N)]$, $i = 0, 1, \dots, (N-1)$. The receiver is the same as the one shown in Figure 4, except that the subcarrier demodulation circuit is an N-ary coherent PSK demodulator. The symbol error probability in this case is given by [7]

$$P = 2Q\left(\sqrt{2\frac{E}{N}} \sin \frac{\pi}{N}\right) \quad (2.4.6)$$

For a specified symbol error probability, (2.4.6) gives the value of the E/N required at the input of the subcarrier demodulation circuit. Since there are N signals, each of the same average power, the signal amplitude is related to the receiver sensitivity in photons/bit by

$$\frac{A^2}{R_s} = N_p \log_2 N G q \eta \quad (2.4.7)$$

where R_s is the signaling rate in symbols/sec, as compared to (2.2.10) for binary ($N=2$) subcarrier modulation. The value of E/N given by (2.4.6) can be used with (2.4.7) and (2.2.7) to give an explicit expression for the receiver sensitivity for N-ary subcarrier modulation.

2.5 Hybrid Systems

It is of interest to generalize the results in the preceding sections to hybrid systems in which there are (M-1) intermediate optical amplifiers between the transmitter and receiver. We consider a system with identical amplifiers, all having the same gain G. The optical noise at the input of the M^{th} optical amplifier, which is the preamplifier at the

receiver, is just M times that at the first amplifier. Thus, the noise at the receiver input has a one sided spectral density of $Mn_{sp}(1-1/G)hf$. It is easily shown that the receiver sensitivity for a hybrid system with M amplifiers is obtained by substituting Mn_{sp} for n_{sp} in the corresponding expression for the sensitivity of a receiver with a single preamplifier. For example, a binary FSK system with M identical amplifiers has a receiver sensitivity at $P_e = 10^{-9}$ given by

$$N_p = 36n_{sp} \frac{M(G-1)}{G} \left[1 + \frac{1}{3} \sqrt{9 + \frac{1}{2}BT + \left[\frac{N_1}{12Mn_{sp}(G-1)} \right]^2} \right] \quad (2.5.1)$$

It can be seen from (2.5.1) that the effect of thermal noise rapidly becomes small as M increases. The thermal noise is expected to be less significant in the presence of a larger amount of optical noise, due to the increased number of in-line amplifiers.

This generalization of receiver sensitivity to systems with several amplifiers does not include the effects of gain saturation of the optical amplifiers due to the accumulation of the amplified spontaneous emission (ASE) optical noise. In the presence of gain saturation, it is more convenient to evaluate the optical signal to noise ratio required at the receiver for a given performance. This ratio is independent of the number of amplifiers in the system and depends only on the sensitivity of a receiver with a single preamplifier, as shown in Chapter 3.

2.6 Discussion

Some prior results in [11], related to the sensitivity of direct detection receivers with an optical preamplifier, have been generalized to include FSK and subcarrier modulation formats. Binary FSK was shown to have a receiver sensitivity that is 3 dB (for small

values of BT) to 2 dB (for large values of BT) poorer compared to OOK. Subcarrier modulation was shown to have receiver sensitivity which has the same functional dependence on system parameters, as the receiver sensitivity for OOK and FSK. However, receiver sensitivity for subcarrier modulation is significantly poorer compared to OOK or FSK for moderate values of BT. For very large values of BT, subcarrier modulation is expected to have a receiver sensitivity comparable to that for OOK or FSK.

A comparison of some of our results, which have been obtained using the Gaussian approximation, with an 'exact' analysis for receiver sensitivity [4], shows that the Gaussian approximation gives a poorer result for the receiver sensitivity, as noted before [4], [9]. We have shown how the error in estimating the receiver sensitivity can be reduced by using simple scale factor corrections.

We also discussed how some of the formulae for receiver sensitivity can be generalized for N-ary modulation schemes, as well as for systems with several amplifiers in tandem.

3.0 Maximum System Gain

In Chapter 2, we calculated the receiver sensitivity of optical amplifier systems with direct detection receivers. Optical amplifier systems have a receiver sensitivity that is significantly better than systems using other methods of signal amplification. [10], [2]. Optical amplifiers have revolutionized signal transmission using optical fibers. Analytical results, computer simulations [5],[15], as well as recent experiments [16] have shown the feasibility of using optical amplifier repeatered systems for communication at multi Gb/s rates over transoceanic distances . It is of interest to explicitly calculate the maximum overall system gain of such systems, since this quantity determines the span of these systems without electronic regeneration. Although there have been recent papers in areas related to the propagation of signal and noise through a chain of optical amplifiers [5], most of the results regarding system gain are obtained by computer simulation. In this Chapter, we present a simple analysis to explicitly calculate the system gain of optical

amplifier systems, for the following two principal cases: 1) Constant signal power at each optical amplifier. 2) Equal spacing between amplifiers, which ensures constant total power (signal plus noise) at each amplifier. The simple formulae derived are useful in understanding the dependence of system gain on the bit rate and the amplifier parameters (gain, bandwidth, noise and linearity); they are also useful in determining the effects of optical filtering at the receiver as well as at the intermediate amplifier stages. Although many of the results in this work related to the calculation of system gain and the dependence on system parameters are implicit in other recent publications, the purpose of this work is to facilitate the understanding of those results by means of simple, yet accurate analytical formulae.

3.1 *Optical Signal To Noise Ratio*

Consider a system having (M-1) identical amplifiers as linear repeaters and an Mth amplifier as a receiver preamplifier, in which the gain of each amplifier compensates for the fiber loss between amplifiers. Assuming that the input to the decision circuit is Gaussian distributed, it can be shown [8] that the receiver sensitivity in photons/bit required to achieve a BER of Q(k), is given by (see Table I for explanation of symbols used in all equations)

$$N_p = 2k^2 n_{sp} M \frac{(G-1)}{G} \left[1 + \frac{1}{k} \sqrt{BT + \left[\frac{N_1}{6n_{sp} M(G-1)} \right]^2} \right] \quad (3.1.1)$$

N_p is the average number of signal photons/bit required at the input of the Mth optical amplifier to achieve the specified BER. The second term in the square root in (3.1.1) is

due to the thermal noise at the receiver, which becomes negligible for moderately large values of M . In a long haul communication system, it can be assumed that amplified spontaneous emission (ASE) is the dominant source of noise, and the receiver sensitivity can be written as

$$N_p = 2k^2 n_{sp} M \frac{(G-1)}{G} \left[1 + \frac{1}{k} \sqrt{BT} \right] \quad (3.1.2)$$

(3.1.1) and (3.1.2) are valid for OOK direct detection systems; similar expressions for the receiver sensitivity can be found using the Gaussian approximation, for other modulation formats (as was done in Chapter 2, for FSK and subcarrier modulation) and methods of detection. (3.1.1) and (3.1.2) are derived assuming that the optical noise is present in the two polarization modes of the fiber. In principle, N_p may be reduced by a factor of two from that given by (3.1.1) and (3.1.2), by the use of a polarization filter at the receiver. The results for receiver sensitivity in Chapter 2 were obtained assuming the presence of such a polarization filter. Here, we do not assume the presence of such a polarization filter in order to make the analysis more general. The validity of using the Gaussian approximation in calculating the receiver sensitivity was also discussed in Chapter 2. It was seen that the values of receiver sensitivity N_p obtained using the Gaussian approximation were reasonably close to those obtained by an ‘exact’ analysis, especially for the case of OOK. Hence, we continue to use the results obtained using the Gaussian approximation, to calculate the optical signal to noise at the receiver.

The receiver sensitivity N_p , given by (3.1.2), is the minimum signal power in photons/bit required at the receiver to achieve a BER of $P_e = Q(k)$. The signal power in Watts is obtained by multiplying N_p by the photon energy hf and the bit rate $R_b = 1/T$. Without a polarization filter at the receiver, the optical noise at the input to the M^{th} amplifier has a spectral density of $2n_{sp}M(1-1/G)hf$, which corresponds to a noise power of $2n_{sp}M(1-1/G)hf B$. Thus, the optical signal to noise ratio required at the input of the M^{th}

amplifier, to achieve a BER of $Q(k)$ is

$$\frac{S}{N} = \frac{N_p(1/T)hf}{2n_{sp}M[(G-1)/G]hfB} = \frac{k^2}{BT} \left[1 + \frac{1}{k} \sqrt{BT} \right] \quad (3.1.3)$$

It should be noted that the optical signal to noise ratio determined by (3.1.3) is independent of the number of amplifiers in the system M . For a given system design, the optical signal to noise ratio given by (3.1.3) determines the maximum number of amplifiers that can be cascaded, and consequently the maximum system gain that can be achieved at a BER of $Q(k)$. For example, consider a system with an optical bandwidth of 2 nm (centered at the transmission wavelength of 1550 nm, which corresponds to $B = 250$ GHz) and $R_b = 1/T = 2.5$ Gb/s. For $P_e = 10^{-15} = Q(7.95)$, the minimum required signal to noise ratio at the receiver is given by (3.1.3) with $BT = 100$ and $k = 7.95$, and is equal to 1.427. In practice, the actual signal to noise ratio required at the receiver will be greater than that given by (3.1.3), to allow for a sufficient margin to compensate for receiver sensitivity penalty incurred due to impairments. These impairments include the effects of dispersion and fiber nonlinearities. The accumulation of ASE noise and the dependence of system gain on system design and amplifier parameters is discussed in the following section, neglecting the effect of impairments mentioned above.

3.2 Analysis For Maximum System Gain

We first consider the “ideal case”, in which the system has M identical amplifiers, each having gain G_0 . The amplifiers are separated by fiber spans of loss L such that $L = 1/G_0$. The signal power at the input of each amplifier is thus $P_R = P_T/G_0$, where P_T is the

signal power at the transmitting end of the system. The optical signal to noise ratio is given by

$$\frac{S}{N} = \frac{P_T}{2n_{sp}M(G_0-1)hfB} = \frac{1}{M\epsilon} \quad (3.2.1)$$

where

$$\epsilon = \frac{2n_{sp}(G_0-1)hfB}{P_T} = \frac{2n_{sp}(G_0-1)BT}{N_T} \quad (3.2.2)$$

Here N_T is the average number of photons/bit at the output of each amplifier, as well as at the input to the fiber at the transmitting end of the system. ϵ is the ratio of the noise power added by one amplifier to the total transmitted power (signal and noise) at the output of each amplifier. In order to achieve a performance of $P_e = Q(k)$, the maximum number of amplifiers M that can be cascaded is determined by equating the signal to noise ratio given by (3.2.1) to the minimum required signal to noise ratio, which is determined by (3.1.3). It follows from (3.1.3) and (3.2.1) that the maximum system gain at a BER of $Q(k)$,

$$\Gamma_0 = G_0^M \quad (3.2.3)$$

is given (in dB) by

$$10 \log \Gamma_0 = \frac{10 \log G_0}{G_0-1} \frac{N_T}{2n_{sp}} \frac{1}{k^2 + k\sqrt{BT}} \quad (3.2.4)$$

For example, consider a system with the parameters $G_0 = 20$ dB (which corresponds to a fiber loss of $L = -20$ dB between amplifiers), $n_{sp} = 1.5$, $B = 5$ nm, $R_b = 1/T = 2.5$ Gb/s, $P_T = 1$ mW. For a BER of $10^{-15} = Q(7.95)$, the minimum required signal to noise ratio at the receiver is given by (3.1.3) with $BT = 250$ and $k = 7.95$, and is equal to 0.756. Equating the signal to noise ratio given by (3.2.1) to 0.756 gives the maximum number of amplifiers that can be cascaded as $M = 55$. The system gain is given by (3.2.4), and is equal to 1100 dB (this can also be obtained from (3.2.3) with $M = 55$ and $G_0 = 20$ dB).

This would correspond to a transmission distance of 4400 km, assuming a fiber loss of 0.25 dB/km. For the same system parameters, if amplifiers with $G_0 = 10$ dB are used, the maximum number of amplifiers increases to 605, which gives a system gain of 6050 dB, corresponding to a transmission distance of 24,200 km! It can be seen that from (3.2.4) that Γ_0 decreases monotonically as G_0 increases from unity. Maximum system gain is obtained with an infinite number of amplifiers with gain infinitesimally greater than unity. Thus, for a fixed set of parameters, maximum achievable system gain increases as the gain of the individual amplifiers decreases.

Effect of optical filter following last amplifier

If there is an optical filter of bandwidth B_0 following the last amplifier, then the optical filter reduces the optical noise power by a factor B_0/B , since the optical noise at the amplifier output is spread over a bandwidth of B . The signal power remains the same since it is assumed that the filter has a bandwidth which is larger than the linewidth of the signal. It follows that the minimum required optical signal to noise ratio at the output of the last amplifier (or at the input of the optical filter) is given by

$$\frac{S}{N} = \frac{B_0}{B} \frac{k^2}{B_0 T} \left(1 + \frac{\sqrt{B_0 T}}{k}\right) = \frac{k^2}{B T} \left(1 + \frac{\sqrt{B_0 T}}{k}\right) \quad (3.2.5)$$

which gives

$$10 \log \Gamma_0 = \frac{10 \log G_0}{G_0 - 1} \frac{N_T}{2n_{sp}} \frac{1}{k^2 + k\sqrt{B_0 T}} \quad (3.2.6)$$

It can be seen from (3.2.6) that the total system gain is dependent only on B_0 , the filter bandwidth, and not on B , the optical bandwidth at each amplifier stage. Consider a system with optical amplifiers whose optical bandwidth is $B = 25$ nm, and with the system

parameters $G_0 = 20$ dB, $n_{sp} = 1.5$, $R_b = 1/T = 2.5$ Gb/s, $P_T = 1$ mW. The maximum system gain, given by (3.2.4) is 600 dB. If we now have an optical filter at the receiver with bandwidth $B_0 = 1$ nm, the system gain, given by (3.2.6) is now 1740 dB. Since the system is presumed linear, filtering need be done only prior to the detector, and does not have to be done at each amplifier. This suggests that the system performance can be greatly improved merely by using a narrowband filter at the receiver. In practice, however, if the bandwidth of each amplifier is large, then ASE can be much larger than the signal. This large ASE will cause the amplifiers to saturate. Thus, particularly when the amplifier bandwidth is large, saturation effects need to be considered.. The preceding analysis has to be extended to include the effects of gain saturation in the optical amplifiers to give more realistic results. We use a “hard” saturation model for the optical amplifiers, to account for gain saturation.

“Hard” saturation amplifier model

The “hard” saturation system model assumes that all the amplifiers are operating deep into saturation and so the total power (signal and noise) at the output of each amplifier is the same. The input and output signal and noise powers at the m^{th} amplifier are shown in Figure 11. From Figure 11, it can be seen that the recursion relations satisfied by the signal and noise as they propagate through the chain of amplifiers are

$$P_{R,m+1} = P_{Rm} G_m L_{m+1} \quad (3.2.7)$$

$$P_{N,m+1} = P_{Nm} G_m L_{m+1} + 2n_{sp} hfB(G_m - 1)L_{m+1} \quad (3.2.8)$$

Since the signal power at the transmitting end of the system is P_T , and the noise at the transmitting end due to the laser transmitter is assumed to be negligible, the initial

conditions for the recursion relations (3.2.7) and (3.2.8) are

$$P_{R1} = P_T L_1 \quad (3.2.9)$$

$$P_{N1} = 0 \quad (3.2.10)$$

with the saturation condition given by

$$P_T = P_{Rm} G_m + P_{Nm} G_m + 2n_{sp} hfB(G_m - 1) \quad (3.2.11)$$

(3.2.11) is based on the assumption that the total power output at each of the amplifiers is same as the signal power transmitted by the laser source into the fiber at the transmitting end of the system. It can be shown from (3.2.7), (3.2.8) and (3.2.11) that the gains of successive amplifiers are related by

$$\frac{G_{m+1}}{G_m} = \frac{1}{\xi_m + \frac{2n_{sp} hfB(1-L_{m+1})G_m}{P_T + 2n_{sp} hfB}} \quad (3.2.12)$$

where

$$\xi_m = G_m L_{m+1} \quad (3.2.13)$$

Assuming that $L_{m+1} \ll 1$ and $2n_{sp} hfB \ll P_T$ (both assumptions are satisfied by practical systems), (3.2.12) can be simplified to

$$\frac{G_{m+1}}{G_m} = \frac{1}{\xi_m + \epsilon \frac{G_m}{G_0}} \quad (3.2.14)$$

where ϵ is given by (3.2.2) and where it is assumed that $G_0 = 1/L_1 \gg 1$. Using the initial conditions (3.2.9) and (3.2.10), the gain of the first amplifier is given by

$$G_1 = \frac{1/L_1 + \epsilon}{1 + \epsilon} \approx \frac{1}{L_1(1 + \epsilon)} \quad (3.2.15)$$

where the second expression in (3.2.15) applies if (as is generally true) $1/L_1 \gg \epsilon$. A closed form solution for the system gain can be readily obtained for the following two

special cases.

Case I

We take $\xi_m = 1$, which implies

$$L_{m+1} = \frac{1}{G_m} \quad (3.2.16)$$

This results, from (3.2.7) in

$$P_{R,m+1} = P_{Rm} = P_{R1} = P_T/G_0 \quad (3.2.17)$$

(3.2.17) implies that the received signal power at each amplifier is equal and, from (3.2.8), assuming that $G_{m-1} \approx G_m$, we get

$$P_{N,m+1} = 2mn_{sp}hfB \quad (3.2.18)$$

From (3.2.17) and (3.2.18), it can be seen that for Case I, (constant signal power at each amplifier, in presence of gain saturation) the S/N is the same as in the absence of saturation and is given by (3.2.1). However, this signal to noise ratio is achieved at the expense of unequal amplifier spacing satisfying (3.2.16). It follows from (3.2.14) that with $\xi_m = 1$

$$\frac{G_{m+1}}{G_m} = \frac{1}{1 + \epsilon \frac{G_m}{G_0}} \quad (3.2.19)$$

It can be shown from (3.2.15) and (3.2.19) that the gain of the m^{th} amplifier is given by

$$G_m = \frac{G_0}{1 + m\epsilon} \quad (3.2.20)$$

It can be seen from (3.2.20) that amplifiers of decreasing gain are required in order to maintain the same amount of signal power in presence of gain saturation; as a result, though the S/N for Case I is the same as in the “ideal” case, there is a reduction in the

overall system gain for Case I as compared to the “ideal” case. This implies that a greater number of amplifiers are required in presence of saturation to achieve the same system gain as the “ideal” case. The total system gain for Case I is given by

$$\Gamma = \prod_{m=1}^M G_m = G_0^M \prod_{m=1}^M \left(\frac{1}{1+m\epsilon} \right) \quad (3.2.21)$$

where M is the maximum number of amplifiers that can be cascaded, determined by (3.2.1). The numerical consequences of the results for Case I are discussed in Section 3.3. We now analyze the case of equal amplifier spacing, which ensures constant total power at the output of each amplifier.

Case II

Now consider the case when the fiber sections are of equal length, that is, $L_m = L_1'$, where the prime is used to indicate that the value of L_1 here is different from that in Case I, if the same signal to noise ratio is to be achieved in both cases. Since all fiber sections are of equal length, we have

$$\xi_m = G_m L_{m+1} = G_m L_1' \quad (3.2.22)$$

and from (3.2.12), we get

$$\frac{G_{m+1}}{G_m} = \frac{1}{G_m L_1' (1+\epsilon')} \quad (3.2.23)$$

where $G_0' = 1/L_1'$, and the prime is similarly used on ϵ to indicate that G_0' is used in the defining equation (3.2.2). It can be shown that the above equations lead to

$$G_m = \frac{1}{L_1(1+\epsilon)} = G_1 = \text{constant} \quad (3.2.24)$$

in which case

$$P_{R,m+1} = \left(\frac{1}{1+\epsilon}\right)^m \frac{P_T}{G_0} \quad (3.2.25)$$

Therefore, the received signal power decays as we go down the amplifier chain. Using the above equations in the recursion equations, it can be shown that

$$P_{NM} + 2n_{sp}hfB = 2n_{sp}hfB \frac{1+\epsilon}{\epsilon} \left[1 - \frac{1}{(1+\epsilon)^M} \right] \quad (3.2.26)$$

from which it follows that the signal to noise ratio is given by

$$\frac{S}{N} = \frac{\{1/(1+\epsilon)\}^M}{1 - \{1/(1+\epsilon)\}^M} \quad (3.2.27)$$

as contrasted with

$$\frac{S}{N} = \frac{1}{M\epsilon} \quad (3.2.28)$$

in Case I. For Case II then, the overall system gain is given by

$$\Gamma = G_0^M = G_1^M (1+\epsilon)^M \quad (3.2.29)$$

where M is the maximum number of amplifiers that can be cascaded, determined by (3.2.27). Note that (3.2.29) is consistent with the definition of system gain as the reciprocal of the overall system loss, since $G_0' = 1/L$. The reduction in maximum achievable system gain due to gain saturation, for Case II, is discussed in Section 3.3.

As mentioned before, if the receiver has an optical filter of bandwidth B_0 , the effect is to reduce the minimum required optical signal to noise ratio (used in (3.2.28) for Case I and in (3.2.27) for Case II, to determine M) at the input to the filter to the one given by (3.2.5); if there is no optical filter at the receiver, the required signal to noise ratio is given

by (3.1.3). However, when gain saturation is taken into account, the system gain is also dependent on B , the optical bandwidth at each amplifier stage (since ϵ is dependent on B). This is so because the amount of saturation of the amplifiers depends on the amount of ASE noise power present at each amplifier, which in turn is dependent on B .

In Case I, the maximum number of amplifiers M is obtained from (3.2.28), while ((3.2.21) gives the total system gain. For Case II, M is obtained from (3.2.27), and (3.2.29) gives the total system gain. The numerical consequences of these equations are discussed in Section 3.3.

3.3 Examples

3.3.1 Gain reduction due to saturation

The system gain for the “ideal” system without any gain saturation in the amplifiers, is given by (3.2.4), or by (3.2.6) if there is an optical filter at the receiver. The maximum number of amplifiers M that can be cascaded in this case is determined from (3.2.1), where the minimum required signal to noise ratio S/N is determined by (3.1.3), or by (3.2.5) if there is optical filtering at the receiver. Gain saturation causes a reduction in the maximum achievable system gain. For Case I, M is determined from (3.2.28), which is same as (3.2.1), which is used to find M for the unsaturated case. Hence, it can be seen from (3.2.21) that the only effect of saturation is to reduce the overall system gain by the factor $\prod_{m=1}^M \{1/(1+m\epsilon)\}$. This is illustrated in Figures 12 and 13, where system gain is plotted as a function of G_0 for two different values of BT . For these examples and all other examples

in this Chapter, we assume the wavelength of the transmitted signal to be 1557 nm, unless indicated otherwise.

It can be seen from (3.1.3) that a given value of BT determines the minimum required signal to noise ratio at the receiver S/N, to achieve a BER of Q(k) (if there is optical filtering at the receiver, S/N is determined from (3.2.5) by a given value of BT and a given value of B_0T). Thus, for a given value of BT, the reduction factor of the system gain for Case I, $\prod_{m=1}^M \{1/(1+m\epsilon)\}$, depends only on the parameter ϵ . The degradation in the maximum achievable system gain due to gain saturation clearly increases for larger values of ϵ . This is intuitive since ϵ is a measure of the amount of noise power added to the system by one amplifier, relative to the total power that is propagated through the system.

To find the effect of gain saturation in Case II, the system gain of Case II, given by (3.2.29), should be compared to the system gain that would have been achieved in the ideal case, which is equal to $(G_0')^{M'}$ where M' is obtained from (3.2.1). This is shown in Figures 14 and 15, for two values of BT. It can be seen from Figures 12 - 15 that the effect of saturation increases for larger BT, for Case I as well as Case II. This is due to the fact that maximum system gain is ultimately limited by the accumulation of ASE noise, which in turn depends on the bandwidth-bit period product BT (more noise power accumulates if the optical bandwidth at each amplifier B is larger).

3.3.2 Comparison of Case I and Case II

The motivation for analyzing Case I is that it achieves the same optical signal to noise ratio in presence of gain saturation, as in the unsaturated or the 'ideal' case. It is interesting to see if Case I gives an advantage over Case II, in terms of the maximum

achievable system gain. Case II is the more practical of the two cases, since it uses identical, equally spaced amplifiers. Figure 16 shows the system gain as a function of G_0 (or G_0' , for Case II) for Cases I and II. It is to be noted that Case I appears to give a larger system gain than Case II for a given value of amplifier gain, but it is achieved at the expense of using a larger number of amplifiers. Note, that in Figure 16 the system gain is plotted as a function of the gain of the first amplifier. However, for Case I, since all the following amplifiers have successively diminishing gain, it is intuitive that Case I will achieve a higher overall gain (since for a system without saturation, it was shown in Section 3.2 that the system gain increases as the gain of an individual amplifier decreases).

A more appropriate way of comparing Cases I and II is to calculate the system gain achievable in both Cases for a fixed value of M , the total number of amplifiers. This is shown in Figure 17. It can be noted that given the value of M , the system gain achieved in Cases I and II is almost identical; in fact, Case I gives a slightly lower gain than Case II. This implies that given a fixed number of amplifiers, no advantage is gained in terms of system gain by adjusting the gains of the amplifiers so as to maintain constant signal power at each amplifier (and the same S/N as in the “ideal” case), over a simple design with identical amplifiers and equal amplifier spacing.

3.3.3 Effect of optical filtering on maximum system gain

It should be noted that Figures 16, 17 are obtained assuming an optical bandwidth of $B = 5$ nm at the output of each amplifier stage. This implies the use of optical filters at each stage since the noise bandwidth of optical amplifiers without any bandpass filtering is considerably larger (≈ 25 nm). There is considerable degradation in the system

performance if the optical filters at each amplifier stage are removed. This is shown in Figures 18 and 19 for Case I and Case II respectively. (Under saturation conditions, the gain vs. wavelength curve of the amplifier changes and there is a peaking of the response around $\lambda = 1.537 \mu\text{m}$ [17]. If the source wavelength is chosen to correspond to this peak, then noise filtering is achieved. In this case, filters may not be required at each amplifier [16].) As mentioned before, the use of an optical filter with a narrow bandwidth B_0 at the receiver can increase the maximum achievable system gain. However, it can be seen from Figures 18 and 19 that the use of a filter at the receiver alone does not greatly improve the maximum achievable system gain. Clearly, the best performance is obtained by a combination of using optical filters at intermediate stages as well as using a narrow bandwidth receiver filter.

3.3.4 Effect of other parameters on maximum system gain

The previous examples have shown the dependence of maximum system gain on amplifier gain and the optical bandwidth at each amplifier stage. In these examples, we assumed a fixed bit rate ($R_b = 2.5 \text{ Gb/s}$) and total power at the output of each amplifier ($P_T = 1 \text{ mW}$). The set of equations in Section 3.2 can also be used to study the dependence of the maximum system gain on the bit rate as well as the total power at the output of each amplifier. If the other parameters are kept constant, the maximum system gain decreases as the bit rate increases, and increases as the propagated power P_T increases. It is shown in Section 3.4 that the total power at the output of each amplifier stage P_T depends on the saturation power P_{sat} of the amplifiers. Consequently, the use of amplifiers with a higher value of P_{sat} give a larger system gain.

We can also get some insight into the functional dependence of system gain on system parameters by looking at the parameter ϵ . Since Case I and Case II give almost identical maximum system gain for a given number of amplifiers M , we can draw inferences about the system performances in both cases from the results of Case I, as long as we consider a fixed number of amplifiers M . From (3.2.28), it can be seen that a smaller value of ϵ allows a larger number of amplifiers to be cascaded to achieve a given signal to noise ratio. As mentioned before, it can be seen from (3.2.21) that for a fixed number of amplifiers M , a smaller value of ϵ gives a higher system gain. We can conclude from these arguments that smaller values of ϵ give a higher system gain for both Cases I and II. From the defining equation (3.2.2) for ϵ , it can then be seen that a larger system gain is achieved for smaller values of n_{sp} and G_0 and a larger value of P_T . For example, Figure 20 shows a plot of the system gain for Case II as a function of P_T , for a fixed set of other system parameters. It can be seen that the system gain scales approximately linearly with P_T , as noted in [18], which discusses the functional dependence of system gain on system parameters for the case of equally spaced amplifiers.

3.4 Computer Simulation For Soft Gain Saturation Model

In Section 3.2, the analysis assumed that the amplifiers were operated deep into saturation, where the the output power at each amplifier was a constant, independent of the input power at that amplifier (hard saturation model). The propagation of signal and noise through a chain of optical amplifiers in various degrees of saturation can be studied using

an implicit formula for the saturated amplifier gain [19], given by

$$G_m = G_m'' \exp\left[\frac{(1-G_m)(P_{Rm}+P_{Nm})}{P_{sat}}\right] \quad (3.4.1)$$

This (“soft saturation”) model has been shown to be accurate for practical lumped optical amplifiers [5]. The degree of saturation of the m^{th} amplifier depends on the ratio $(P_{Rm}+P_{Nm})/P_{sat}$. The recursion equations (3.2.7), (3.2.8) and the initial conditions (3.2.9), (3.2.10) can be used with (3.4.1) to give the signal and noise powers at each amplifier stage [5]. The optical signal to noise ratio at the output of the m^{th} amplifier is

$$\frac{S}{N} = \frac{G_m P_{Rm}}{G_m P_{Nm} + 2n_{sp}hfB(G_m-1)} \quad (3.4.2)$$

A computer program has been written, which computes the saturated gain and the signal and noise powers at the output of each amplifier. The simulation terminates when the signal to noise ratio degrades to the minimum required value given by (3.1.3), or (3.2.5) if there is optical filtering at the receiver. The amplifier stage M at which the simulation terminates gives the maximum number of amplifiers that can be cascaded to achieve a given performance. The total system gain is simply the reciprocal of the total fiber loss of the M fiber sections. The methodology of this computer simulation is the same as that followed in [5]. In [5], the emphasis is on showing how a simple lumped amplifier model is accurate in modeling the propagation of signal and noise through a chain of EDFAs. The same amplifier model (3.4.1), and recursion relations (3.2.7), (3.2.8), have been used here; however, the main purpose of the computer simulation in this work is to verify some of the assumptions used in the analysis for calculating the maximum system gain, as well as some of the analytical results, obtained in Section 3.2.

Consider a chain of amplifiers, all having the same unsaturated gain G'' and separated by fiber spans of equal loss L such that $G''L = \alpha$. Figure 21 shows the propagation of signal and noise through the chain of amplifiers for $\alpha = 3$. In Figure 22,

the saturated gain at each stage is plotted as a function of amplifier stage. It can be seen that the gain as well as the total power at the output of each amplifier quickly reach a constant value after a few amplifier stages. Thus, the “hard” saturation assumptions of the previous analysis are accurate as long as the number of amplifier stages is large enough for “hard” saturation to set in. Under these conditions, the saturated gain of each amplifier will be approximately equal to $1/L$ since the loss of each fiber section is compensated by the saturated gain of the following amplifier. It follows that

$$G_m \approx \frac{G''}{\alpha} \quad (3.4.3)$$

The total power (signal and noise) P_{tot} at the output of each amplifier can then be obtained from the implicit gain formula (3.4.1). It can be seen from (3.4.1) that P_{tot} is given by

$$P_{tot} \approx P_{sat} \ln \alpha \quad (3.4.4)$$

Thus, the analytical results (of Case II) in the previous section can be used to calculate M using (3.2.28) and the overall system gain using (3.2.29), if we use the saturated gain given by (3.4.3) as G_0 in (3.2.29), and the total power at each amplifier P_{tot} , given by (3.4.4), as P_T in the defining equation (3.2.2). Since an increase in P_T leads to an improvement in the maximum system gain, the use of amplifiers with a higher P_{sat} give a larger overall system gain. It can be seen from (3.4.3) and (3.4.4) that as α becomes large, G_m decreases and P_{tot} increases, both of which increase the maximum gain. However, this is achieved at the expense of using more amplifiers, since a larger α corresponds to a smaller distance between successive amplifiers. For example, consider a system with a chain of identical amplifiers of unsaturated gain G'' , separated by fiber sections of equal loss L such that $G''L = 3$. Figure 23 shows the maximum system gain obtained by computer simulation, as well as by the analytical results as discussed above (with $P_{tot} = P_T$ and $G_m = G_0$), as a function of the amplifier gain (saturated).

3.5 Effect Of Output Power Variations

In the previous sections, results for the maximum achievable system gain were obtained for two cases: Case I- Constant signal power at each amplifier. Case II- Constant amplifier spacing, which gives constant total power at each amplifier. Case II is the more practical of these two cases, since it has equal amplifier spacing and uses identical amplifiers. The analysis for Case II assumed a constant total power at the output of each amplifier. However, in a practical system, it will be difficult to maintain exactly the same total power at the output of each amplifier. The difficulty arises mainly because of variations of amplifier parameters such as gain G and saturation power P_{sat} . For an ideal linear system with identical, equally spaced amplifiers, it has been shown [11] that variations in the gain and power at each amplifier can severely reduce the maximum achievable system gain.

We extend the analysis in [11] to study the effect of variations in the power at the output of each amplifier in reducing the maximum achievable system gain, in the presence of gain saturation of the amplifiers. Consider a system with M (nominally) identical, equally spaced amplifiers, such that the output power at each amplifier varies around a nominal value P_T , due to parameter variations in the amplifiers. To make the analysis tractable, it is assumed that the total power (signal and noise) at the output of the m^{th} amplifier $P_{T,m}$ is given by

$$P_{T,m} = P_T(1+x_m) \quad m = 1,2,\dots,M \quad (3.5.1)$$

where x_m , $m=1, 2, \dots, M$ are independent, identically distributed Gaussian random variables with zero mean and variance σ^2 . Since the power output at each amplifier is a random variable, the recursion equations (3.2.7), (3.2.8) and the saturation condition (3.2.11) are obtained by replacing the constant P_T in these equations with the random

variable $P_T (1 + x_m)$. In the presence of output power variations, the recursion relations are

$$P_{R,m+1} = P_{Rm} G_m L_{m+1} \quad (3.5.2)$$

$$P_{N,m+1} = P_{Nm} G_m L_{m+1} + 2n_{sp}hfB(G_m-1)L_{m+1} \quad (3.5.3)$$

with the initial conditions

$$P_{R1} = P_T L_1 \quad (3.5.4)$$

$$P_{N1} = 0 \quad (3.5.5)$$

The saturation conditions are given by

$$P_{T,m} = P_T(1+x_m) = P_{Rm} G_m + P_{Nm} G_m + 2n_{sp}hfB(G_m-1) \quad (3.5.6)$$

It can be seen from the equations (3.5.2) - (3.5.6) that the signal power and the noise power at each amplifier are random variables. We define the optical signal to noise ratio at the input of the receiver in this case [11] to be

$$\frac{S}{N} = \frac{E(S)}{\sqrt{\text{var}(S)+E^2(N)}} = \frac{E(P_{R,m+1})}{\sqrt{\text{var}(P_{R,M+1})+E^2(P_{N,M+1})}} \quad (3.5.7)$$

where the variation in signal power is treated as an additional source of noise. The variation of the noise power, $\text{var}(P_{N,m+1})$ is neglected, since it is small compared to the squared average noise power $E^2(P_{N,m+1})$.

To achieve a given performance of $P_e = Q(k)$, the signal to noise ratio defined by (3.5.7) must be equal to the minimum required signal to noise ratio at the receiver, determined by (3.1.3). The maximum number of amplifiers that can be cascaded M is thus determined by equating the the signal to ratio defined by (3.5.7) to the the minimum required signal to noise ratio given by (3.1.3). The maximum system gain of the system in the presence of power variations is simply $(G_0)^M$, where $G_0 = 1/L$.

The first step is to find the signal to noise ratio defined by (3.5.7). It can be seen from (3.5.2) - (3.5.6) that in the presence of power variations, the gains of successive amplifiers are related by

$$\frac{G_{m+1}}{G_m} = \frac{(1+x_{m+1})}{(1+x_m)} \left\{ \frac{1}{\xi_m + \left(\frac{\epsilon}{1+x_m} \right) \frac{G_m}{G_0}} \right\} \quad (3.5.8)$$

where $G_0 = 1/L_1$ and $\xi_m = G_m L_{m+1}$, as compared to (3.2.12) in the absence of power variations. It can also be easily shown that the gain of the first amplifier is given by

$$G_1 = \frac{(1+x_1)}{L_1(1+\epsilon)} \quad (3.5.9)$$

For equal amplifier spacing, $L_m = L_1 = 1/G_0$. From (3.2.8) and (3.2.9), it can be seen that when the spacing between the amplifiers is equal, the gain of the $(m+1)^{\text{th}}$ amplifier is given by

$$G_{m+1} = \frac{(1+x_{m+1})}{(1+x_m)} \left\{ \frac{1}{L_1 \left(1 + \frac{\epsilon}{1+x_m} \right)} \right\} \quad (3.5.10)$$

Using (3.5.9) and (3.5.10) in the recursion relations (3.5.2) - (3.5.6), it follows that the signal power at the $(m+1)^{\text{th}}$ amplifier is given by

$$S = P_{R,m+1} = \frac{P_T}{G_0} \frac{(1+x_m)}{(1+\epsilon) \left(1 + \frac{\epsilon}{1+x_1} \right) \left(1 + \frac{\epsilon}{1+x_2} \right) \dots \left(1 + \frac{\epsilon}{1+x_{m-1}} \right)} \quad (3.5.11)$$

From the saturation condition (3.5.6), it can be seen that the noise power at the $(m+1)^{\text{th}}$ amplifier is given by

$$N = P_{N,m+1} = \frac{P_T}{G_0} \left\{ (1+x_m) \left(1 + \frac{\epsilon}{1+x_m} \right) \right\} - P_{R,m+1} \quad (3.5.12)$$

In (3.5.11), assuming $x_i < 1$, $i = 1, 2, \dots, M$, we can use the equality

$$\frac{1}{1+x_i} = 1 - x_i + x_i^2 - x_i^3 + \dots \quad (3.5.13)$$

Using (3.5.13), it can be shown that (3.5.11) can be written as

$$S = P_{R,m+1} = \frac{P_T(1+x_M)^{M-1}}{G_0(1+\epsilon)^M} \prod_{j=1}^{M-1} \left\{ 1 + \sum_{i=1}^{\infty} \left\{ (-1)^i (x_j)^i \left[\frac{1}{(1+\epsilon)^i} - \frac{1}{(1+\epsilon)^{i-1}} \right] \right\} \right\} \quad (3.5.14)$$

Since the random variables x_i $i = 1, 2, \dots, M$, are assumed to be independent and hence uncorrelated, all powers of x_i , $(x_i)^k$ are also independent and uncorrelated [20]. It follows that the mean value of the signal power is given by the product of the means of the terms containing x_1, x_2, \dots, x_M . This gives

$$S = P_{R,m+1} = \frac{P_T}{G_0(1+\epsilon)^M} \prod_{j=1}^{M-1} E \left\{ 1 + \sum_{i=1}^{\infty} \left\{ (-1)^i (x_j)^i \left[\frac{1}{(1+\epsilon)^i} - \frac{1}{(1+\epsilon)^{i-1}} \right] \right\} \right\} \quad (3.5.15)$$

Since the x_i $i = 1, 2, \dots, M$, are identically distributed and have the same variance σ^2 , (3.5.15) simplifies to

$$S = P_{R,m+1} = \frac{P_T}{G_0(1+\epsilon)^M} \left\{ E \left\{ 1 + \sum_{i=1}^{\infty} \left\{ (-1)^i (x_j)^i \left[\frac{1}{(1+\epsilon)^i} - \frac{1}{(1+\epsilon)^{i-1}} \right] \right\} \right\} \right\}^M \quad (3.5.16)$$

Since x_i $i = 1, 2, \dots, M$, are zero mean Gaussian random variables, the moments of x_i are given by [20]

$$E[(x_i)^n] = \begin{cases} 1 \times 3 \times \dots (n-1) \sigma^n & n \text{ even} \\ 0 & n \text{ odd} \end{cases} \quad (3.5.17)$$

Using (3.5.17) in (3.5.16), we get

$$E(S) = \frac{P_T}{G_0(1+\epsilon)^M} \left\{ 1 + \sigma^2 \left[\frac{1}{(1+\epsilon)^2} - \frac{1}{(1+\epsilon)} \right] + 3\sigma^4 \left[\frac{1}{(1+\epsilon)^3} - \frac{1}{(1+\epsilon)^2} \right] + \dots \right\}^{M-1} \quad (3.5.18)$$

Since σ^2 is usually smaller than 1 for moderate amounts of power variation, we consider only the σ^2 term in the infinite expansion in (3.5.18), which gives

$$E(S) \approx \frac{P_T}{G_0(1+\epsilon)^M} \left\{ 1 + \sigma^2 \left[\frac{1}{(1+\epsilon)^2} - \frac{1}{(1+\epsilon)} \right] \right\}^{M-1} \quad (3.5.19)$$

From (3.5.12), it can be seen that the average noise power is given by

$$E(N) = \frac{P_T}{G_0}(1+\epsilon) - E(S) \quad (3.5.20)$$

where $E(S)$ is given by (3.5.19).

Following a methodology similar to that for obtaining $E(S)$, it can be shown that the mean square value of the signal power $E(S^2)$ is

$$E(S^2) \approx \left(\frac{P_T}{G_0}\right)^2 \frac{1}{(1+\epsilon)^{2M}} \left\{ 1 + \sigma^2 \left[1 - \frac{4}{(1+\epsilon)} + \frac{3}{(1+\epsilon)^2} \right] \right\}^{M-1} \quad (3.5.21)$$

The signal to noise ratio defined by (3.5.7) is given by

$$\frac{S}{N} = \frac{E(S)}{\sqrt{E(S^2) - E^2(S) + E^2(N)}} \quad (3.5.22)$$

where $E(S)$ is given by (3.5.19), $E(N)$ is given by (3.5.20), and $E(S^2)$ is given by (3.5.21). It can be seen from (3.5.21) and (3.5.19) that for $\sigma^2 = 0$, $E(S^2) = E^2(S)$ and consequently, the right hand side of (3.5.22) reduces to $E(S)/E(N)$. From (3.5.19) and (3.5.20) it can be seen that the ratio $E(S)/E(N)$ for $\sigma^2 = 0$ is the same as the right hand side in (3.2.27), which is the signal to noise ratio for Case II in absence of any output power variation.

To observe the effect of power variation in reducing the maximum available system gain, the maximum achievable gain in absence of power variations, which we call the nominal system gain, should be compared to the maximum achievable system in the presence of output power variations. For a given amplifier spacing L or the corresponding G_0 , which is equal to $1/L$, the nominal system gain is $(G_0)^{M'}$, where M' is the maximum number of cascable amplifiers determined from (3.2.27). The system gain in presence of power variation is obtained by equating the $(G_0)^M$, where M is the maximum number of cascable amplifiers determined by equating the signal to noise ratio in (3.5.22) to the

minimum required signal to noise ratio at the receiver, which is determined by (3.1.3) (or by (3.2.5), in the presence of a receiver filter). Figure 24 shows a plot of the nominal system gain and the reduced system gain (due to power variations), as a function of G_0 , for $\sigma = 0.26$, which corresponds to a rms variation of 1 dB in the output power at each amplifier. It can be seen from the figure that a moderate variation in the output power at each amplifier does not cause any significant decrease in the overall achievable system gain. In the presence of gain saturation, there is a self regulating effect [5], in which subsequent amplifiers will tend to correct for parameter variations in preceding amplifiers. As a result, the system can withstand the effect of moderate amounts of parameter variations.

3.6 Discussion

We have obtained analytical results to explicitly calculate the maximum achievable system gain of linear systems with optical amplifiers. Gain saturation in optical amplifiers is shown to decrease the maximum achievable system gain. We have shown that in presence of gain saturation, nearly identical system gain is achieved with a fixed number of amplifiers, for the following two cases : 1) Constant signal power at each amplifier. 2) Equal amplifier spacing, with identical amplifiers. Optical filtering at the receiver decreases the minimum required optical signal to noise ratio at the receiver and consequently gives an improvement in the maximum achievable system gain. However, we have shown that in presence of gain saturation, the maximum achievable gain also depends on the optical noise bandwidth at each amplifier stage. The assumptions used in the analysis have been shown to be valid through computer simulation of signal and noise propagation.

The main contribution of this Chapter is the simple analytical formulae that have been derived which show the functional dependence of the maximum achievable system gain on system parameters. These formulae can also be used for the explicit calculation of the overall system gain for a set of system parameters. For example, consider a system with identical, equally spaced amplifiers. Let $G'' = 13$ dB, $L = -10$ dB (this implies that $G''*L = \alpha \approx 2$ and that the saturated gain $G = G_0 \approx 10$ dB), $P_{\text{sat}} = 1.6$ dBm (this gives $P_T \approx 1$ mW), $R_b = 1/T = 5$ Gb/s, $B = 5$ nm (optical filtering at each amplifier stage), $n_{\text{sp}} = 2$. For a probability of error 10^{-9} ($k=6$), the minimum required optical S/N at the receiver, given by (3.1.3), is 0.82. The maximum number of amplifiers that this system can have, given by (3.2.27), is 275. The overall system gain, given by (3.2.29), is 2,750 dB. If the fiber loss is assumed to be 0.25 dB/km, this system gain corresponds to an achievable transmission distance of 11,000 km. These analytical results are in good agreement with the results obtained by computer simulation in [15], and the experimental results in [16], in which the respective systems had parameter values close to those assumed in this example. In [15], the maximum number of amplifiers that could be cascaded was computed to be 292, which corresponds to an achievable transmission distance of approximately 12,000 km. In [16], the experiment had an equivalent (since the experiment used a circulating loop) cascade of 300 amplifiers and achieved a transmission distance of 9,000 km. (Due to excess losses in the loop, the transmission distance achieved was less than that calculated taking into account only fiber loss).

The system gain can be increased by operating at a lower bit rate. In the above example, if the bit rate is reduced to 2.4 Gb/s, the maximum number of amplifiers that can be cascaded increases to 375 and the achievable system gain increases to 3,750 dB, corresponding to a transmission distance of 15,000 km. However, it should be noted that a larger bit rate - length product is achieved when operating at the higher bit rate of 5 Gb/s.

If we operate at 5 Gb/s but remove the optical filters at each amplifier stage, (this implies $B \approx 25$ nm), there is considerable degradation in system performance. The maximum number of amplifiers that can be cascaded decreases to 102 and the system gain decreases to 1,020 dB, corresponding to a distance of 4,080 km. A longer transmission distance can be achieved by using optical amplifiers with a higher P_{sat} . With a P_{sat} of 7.6 dB (which gives a P_T of 4 mW), the maximum number of amplifiers increase to 410, corresponding to a gain of 4,100 dB (16,400 km). These results are consistent with those in [15], which are obtained by computer simulations.

The numerical results show that the system gain can be increased by using amplifiers with a lower saturated gain and higher saturation power (and a lower noise coefficient n_{sp}). The overall gain can also be improved by optical filtering at intermediate stages and also by the use of an optical filter at the receiver. Finally, it is to be noted that the analytical results can also be used to study the tradeoffs between different system parameters in achieving a fixed system gain, corresponding to a desired transmission distance.

We have also analyzed the effect of random variations in the total power at the output of each amplifier in reducing the maximum system gain. It was shown that power variations do not significantly degrade the system performance when the amplifiers are operated in saturation.

4.0 Conclusions

We have analyzed two specific problems related to communication systems using optical amplifiers: 1) Receiver sensitivity. 2) Maximum system gain of optical amplifier systems. The methodology for finding analytic expressions for receiver sensitivity using the Gaussian approximation was discussed in Chapter 2. Explicit formulae have been derived for the receiver sensitivity of binary FSK and subcarrier modulation systems. The receiver sensitivity for binary FSK has been shown to be 2 to 3 dB poorer than that for OOK. Subcarrier modulation has been shown to have a receiver sensitivity that is significantly poorer compared to OOK or FSK modulation. The receiver sensitivity results for OOK and binary FSK obtained using the Gaussian approximation have been compared to those obtained by a published 'exact' analysis. It has been shown that the receiver sensitivity obtained using the Gaussian approximation can be made close to the 'exact' receiver sensitivity, especially for large values of the amplifier bit-period bandwidth product

BT (which are of practical interest). It should be noted however, that the validity of using the Gaussian approximation for obtaining the receiver sensitivity in the case of subcarrier modulation has not been addressed in this thesis. However, for large values of BT, where many independent samples of the noise are averaged, the Gaussian approximation should be good. This is a topic for possible future work. The use of optical amplifiers in subcarrier modulation systems is of particular interest for analog video transmission.

The results for receiver sensitivity obtained in Chapter 2 have been used in the analysis in Chapter 3 to find explicit formulae for the optical signal to noise ratio and the resulting maximum system gain of a system having a chain of optical amplifiers. The results give insight into the functional dependence of the maximum system gain on system parameters. The results for the maximum system gain have been shown to agree well with those obtained by numerical computations. The analysis for maximum system gain has also been extended to include the effects of random output power variations at intermediate amplifier stages. The analysis does not however, take into account the effects of other practical impairments such as non-ideal gain profiles of optical amplifiers, fiber nonlinearities and dispersion, in reducing system performance.

Future work along this direction could possibly include the modeling and analysis of the effect of practical impairments which affect system performance. The results in this thesis could also be generalized for multiuser optical fiber networks.

Table I

List of Symbols used

A	Signal amplitude
B	Optical bandwidth at each amplifier stage
B_e	bandwidth of electrical bandpass filter
B_o	Optical bandwidth of filter at receiver
f	Optical frequency
f_s	Subcarrier frequency
G	Amplifier gain
G_m	Saturated gain of m^{th} amplifier
G_m''	Unsaturated gain of m^{th} amplifier
h	Planck's constant
I	Current at the input of the decision circuit
k	Argument of Q function
L_m	Length of m^{th} fiber section
m	Optical modulation index
M	Number of amplifiers
n(t)	Thermal noise at the receiver
N_1	Receiver sensitivity for unity gain
N_p	Receiver sensitivity in photons/bit
n_{sp}	Spontaneous emission coefficient
P_e	Probability of error
P_r	Average power at the receiver
P_{Rm}	Signal power at the input to m^{th} amplifier
P_{Nm}	Noise power at the input to m^{th} amplifier
P_{tot}	Total power at the input to m^{th} amplifier
P_T	Power transmitted at fiber input
q	Electronic charge
Q(k)	Gaussian error probability function
R_b	Bit rate
S/N	Optical signal to noise ratio
T	Bit period

$x(t)$	Inphase component of optical noise
$y(t)$	Quadrature component of optical noise
Z	Effective noise impedance of electrical receiver
Γ	System gain
κ	Boltzmann's constant
σ_{oa}^2	Variance of $x(t), y(t)$
σ_n^2	Variance of $n(t)$
η	Quantum efficiency of photodetector
ω_s	Subcarrier radian frequency

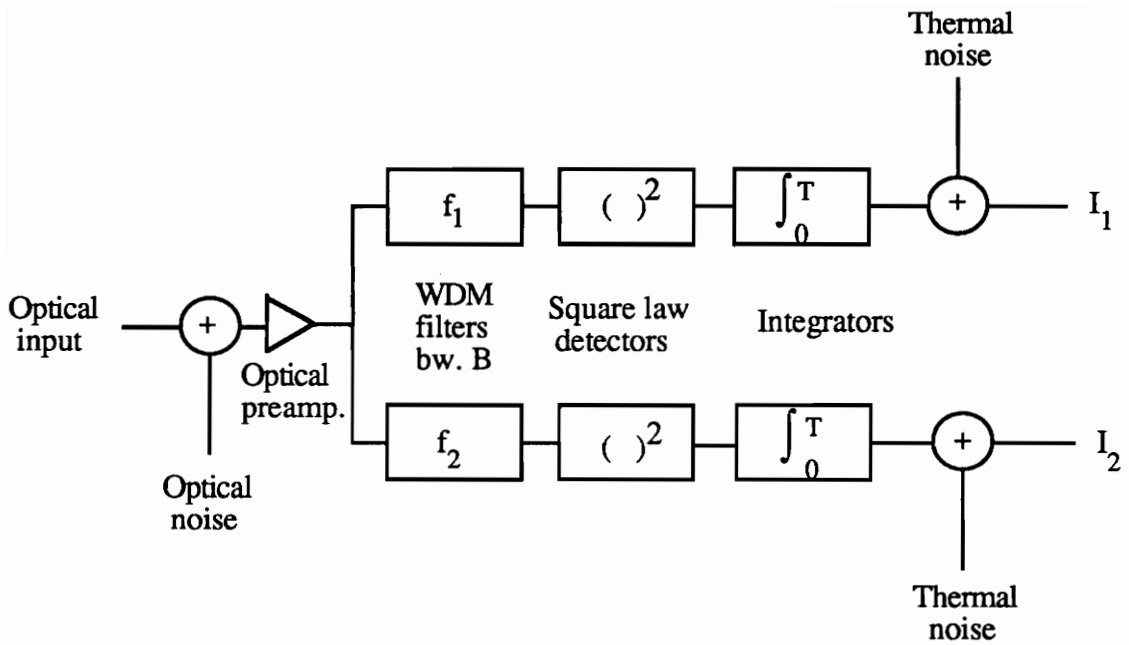


Figure 1. Receiver model for binary FSK system.

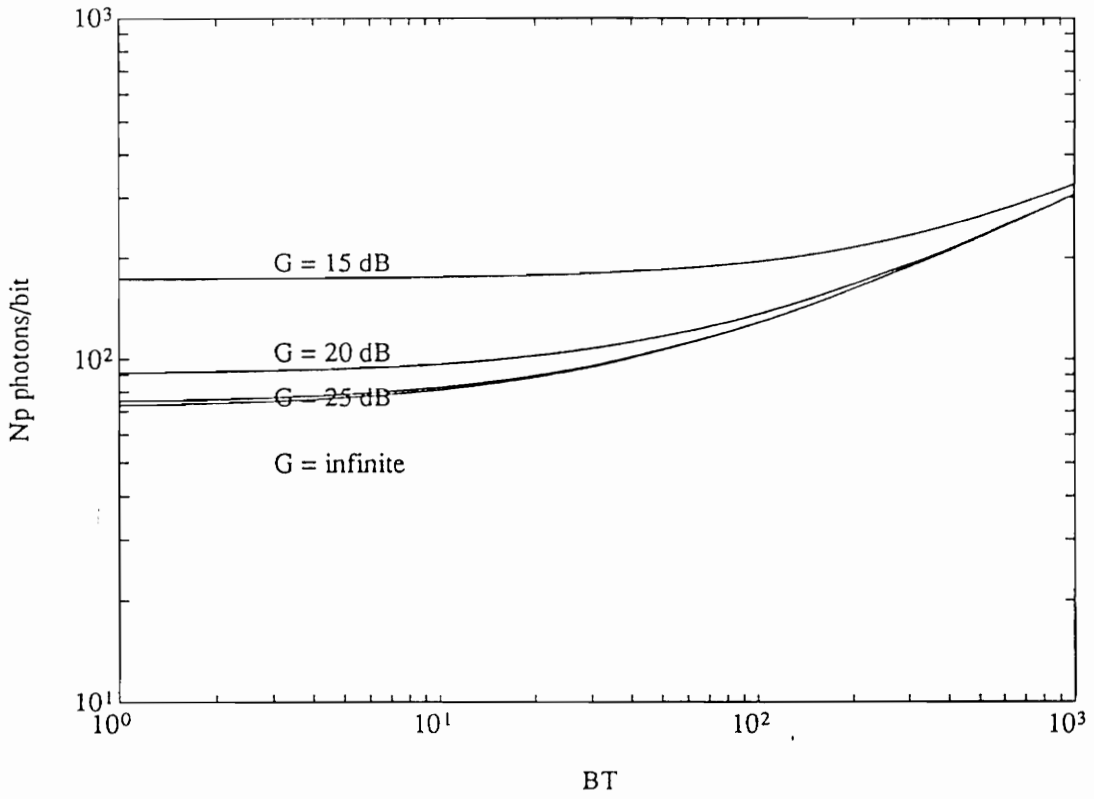


Figure 2. Receiver sensitivity for binary FSK for different values of amplifier gain. $N_1 = 4200$ photons/bit, $n_{sp} = 1$.

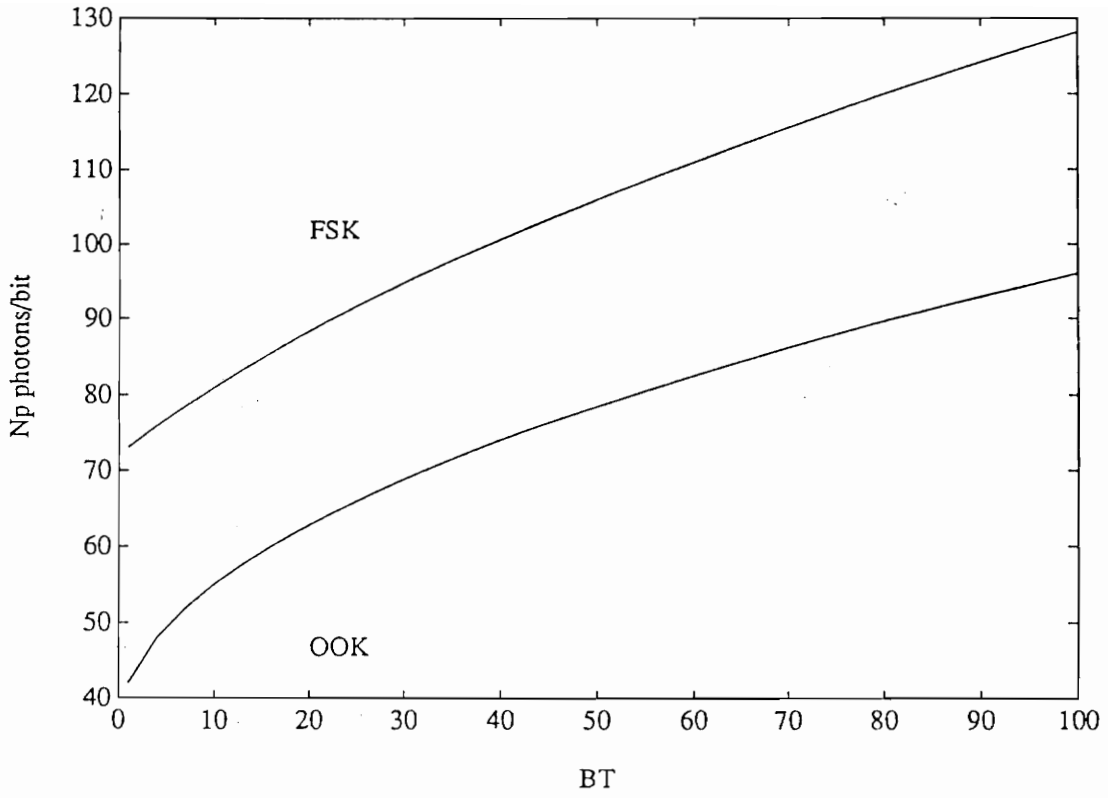


Figure 3. Comparison of receiver sensitivity for binary FSK and OOK for large values of amplifier gain. $n_{sp} = 1$.

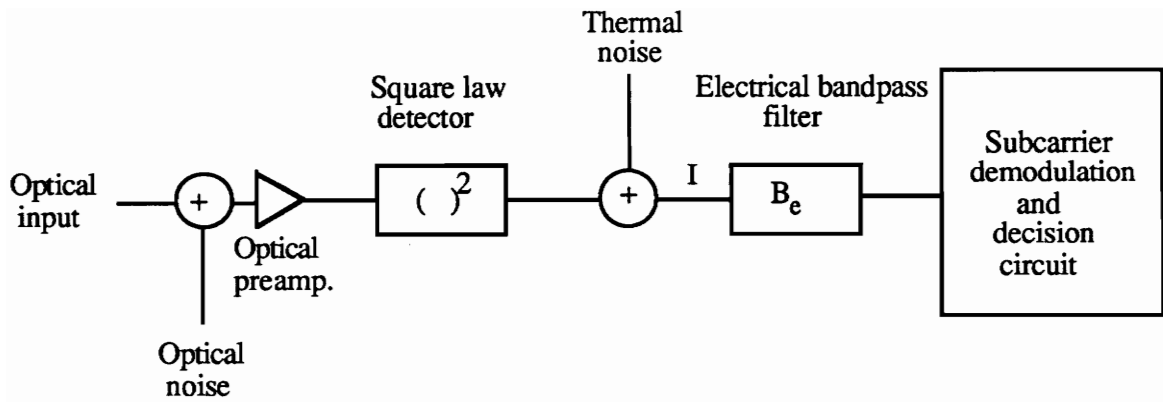


Figure 4. Receiver model for binary subcarrier modulation system.

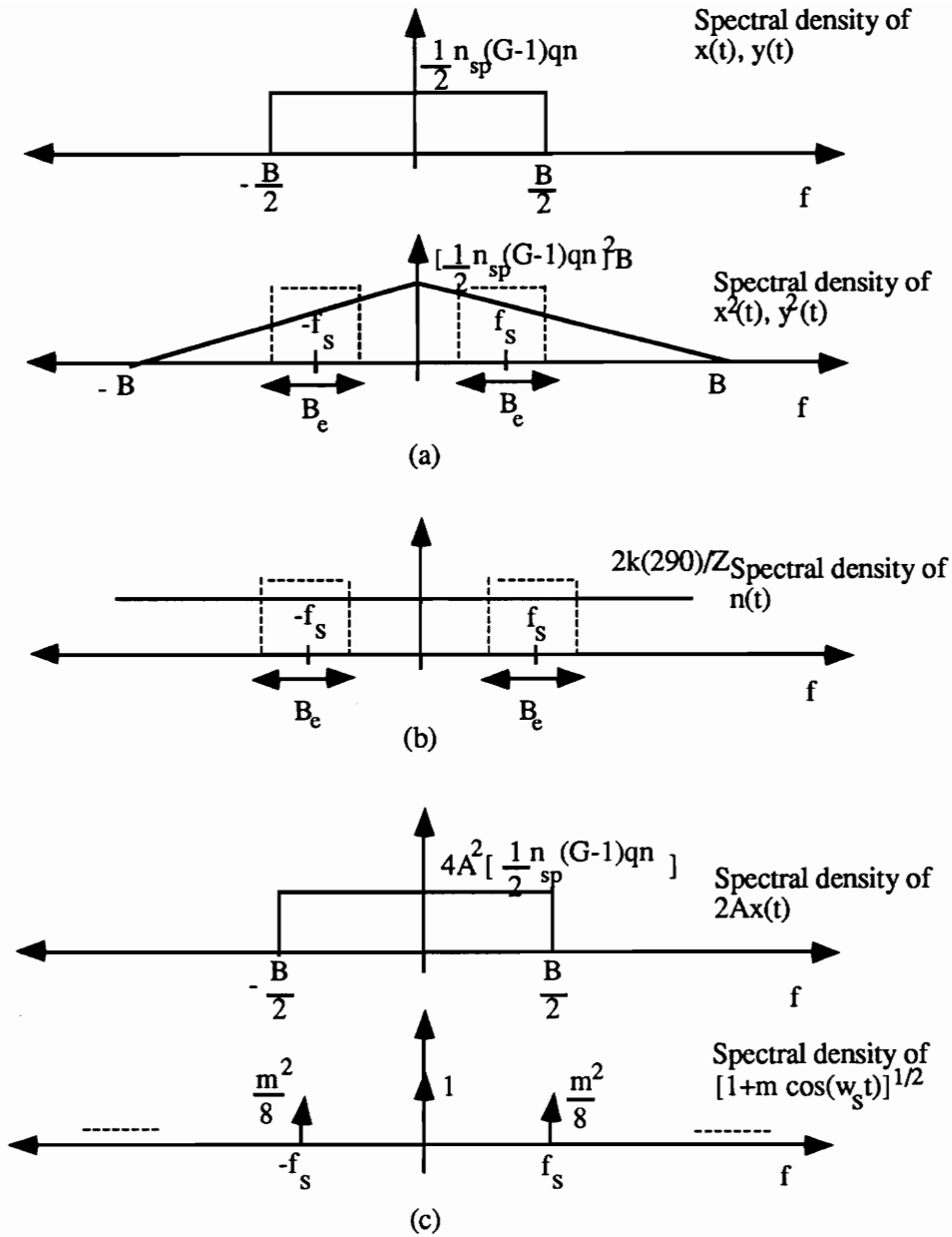


Figure 5(a). Noise power due to $x^2(t), y^2(t)$.
 Figure 5(b). Noise power due to $n(t)$.
 Figure 5(c). Noise power due to $2A[1+m \cos(w_s t)]^{1/2} x(t)$

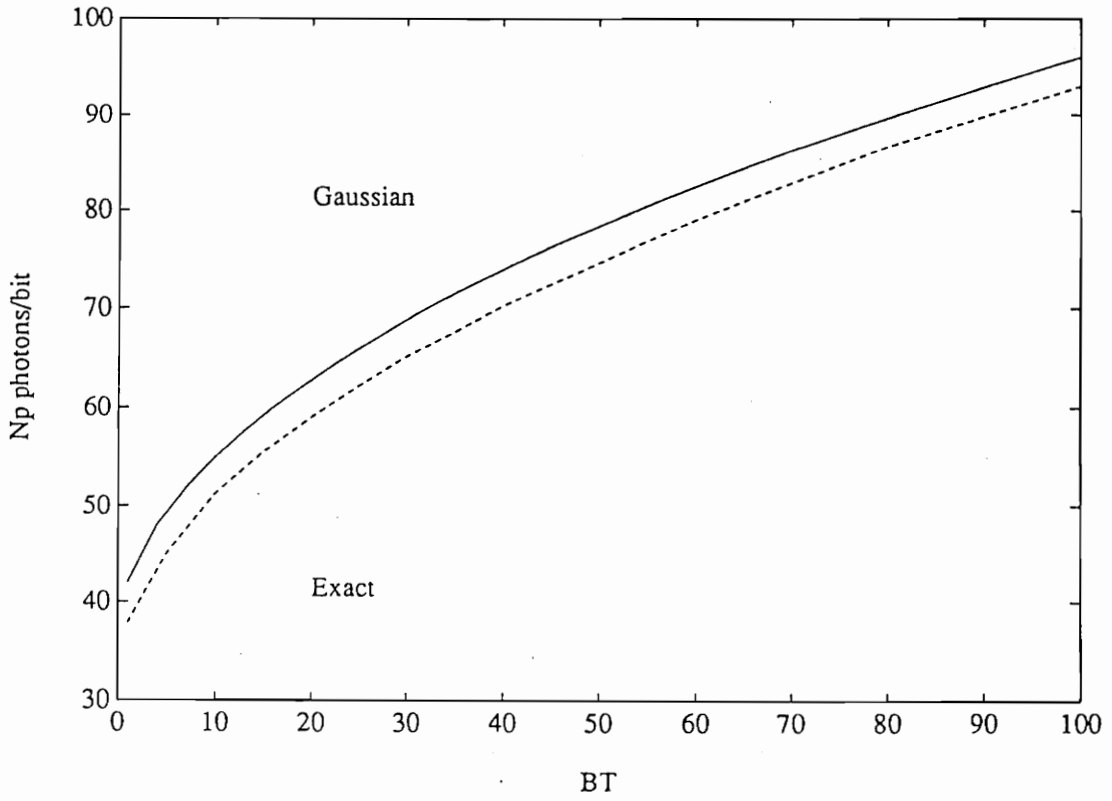


Figure 6. Comparison of receiver sensitivity obtained using Gaussian approximation with 'exact' receiver sensitivity [4], with $k=6$.

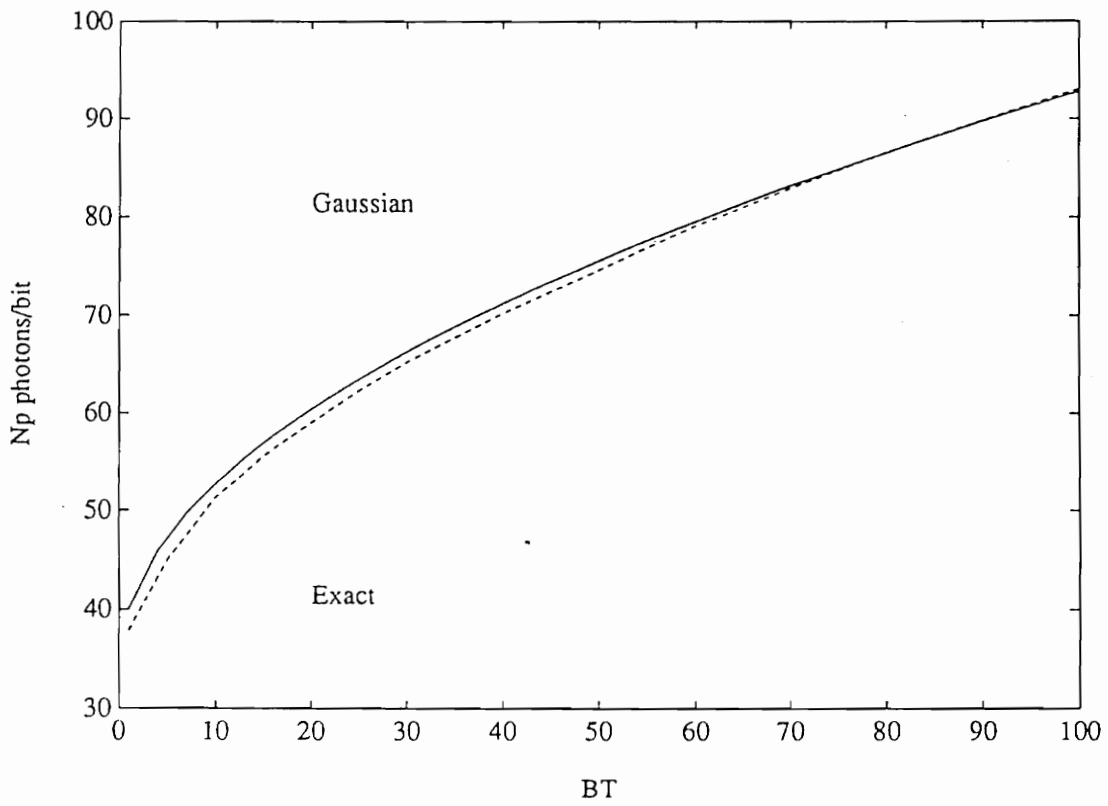


Figure 7. Comparison of receiver sensitivity obtained using Gaussian approximation with 'exact' receiver sensitivity [4], with $k' = 5.85$ (using correction factor).

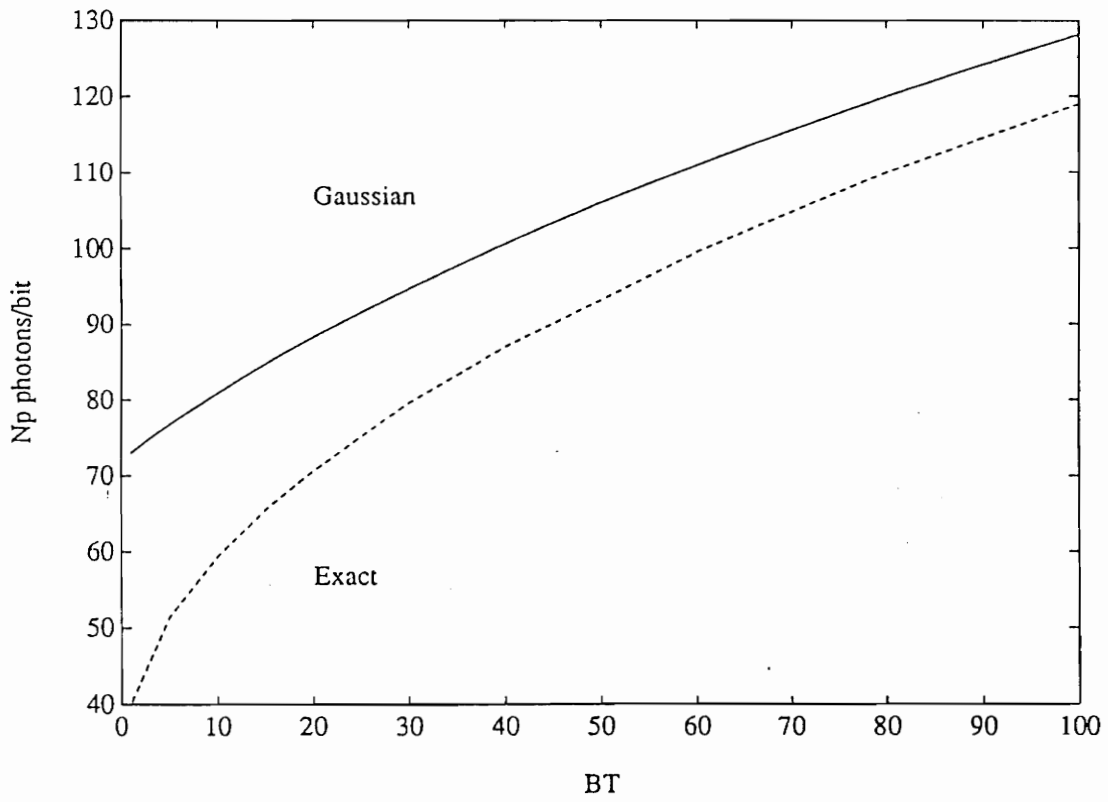


Figure 8. Comparison of receiver sensitivity obtained using Gaussian approximation with 'exact' receiver sensitivity [4] for FSK, with $k = 6$.

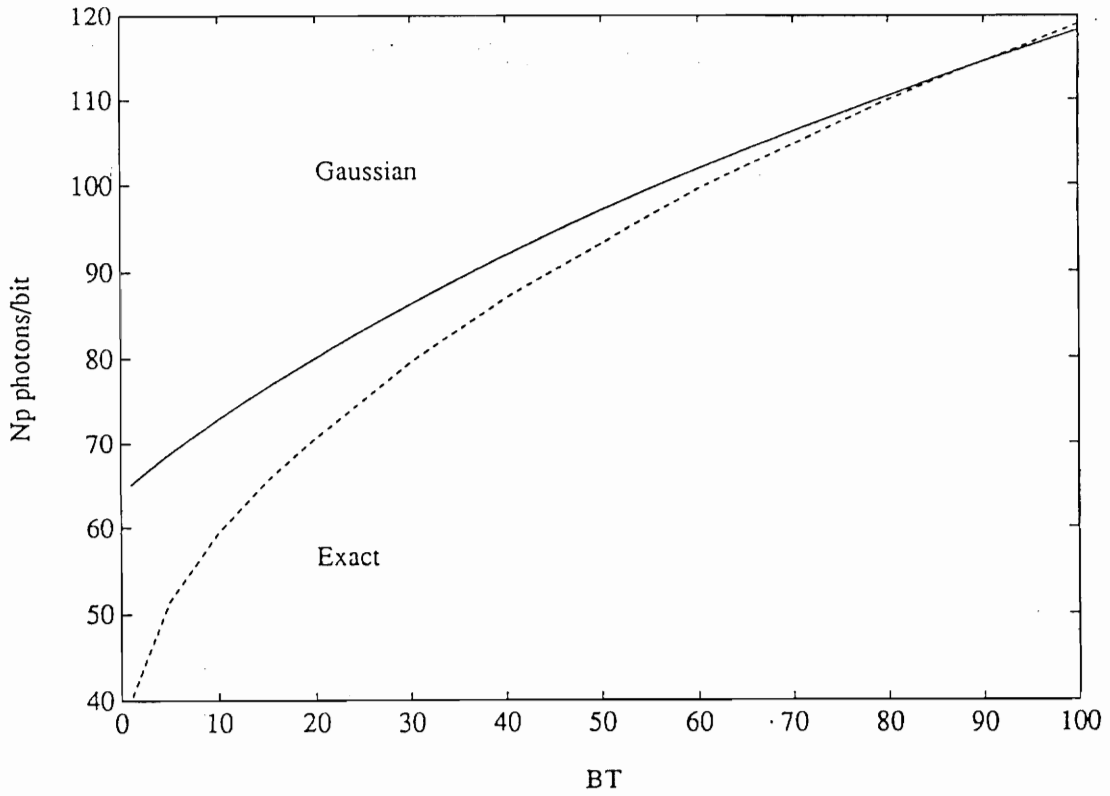


Figure 9. Comparison of receiver sensitivity obtained using Gaussian approximation with 'exact' receiver sensitivity [4] for FSK, with $k' = 5.65$ (using correction factor).

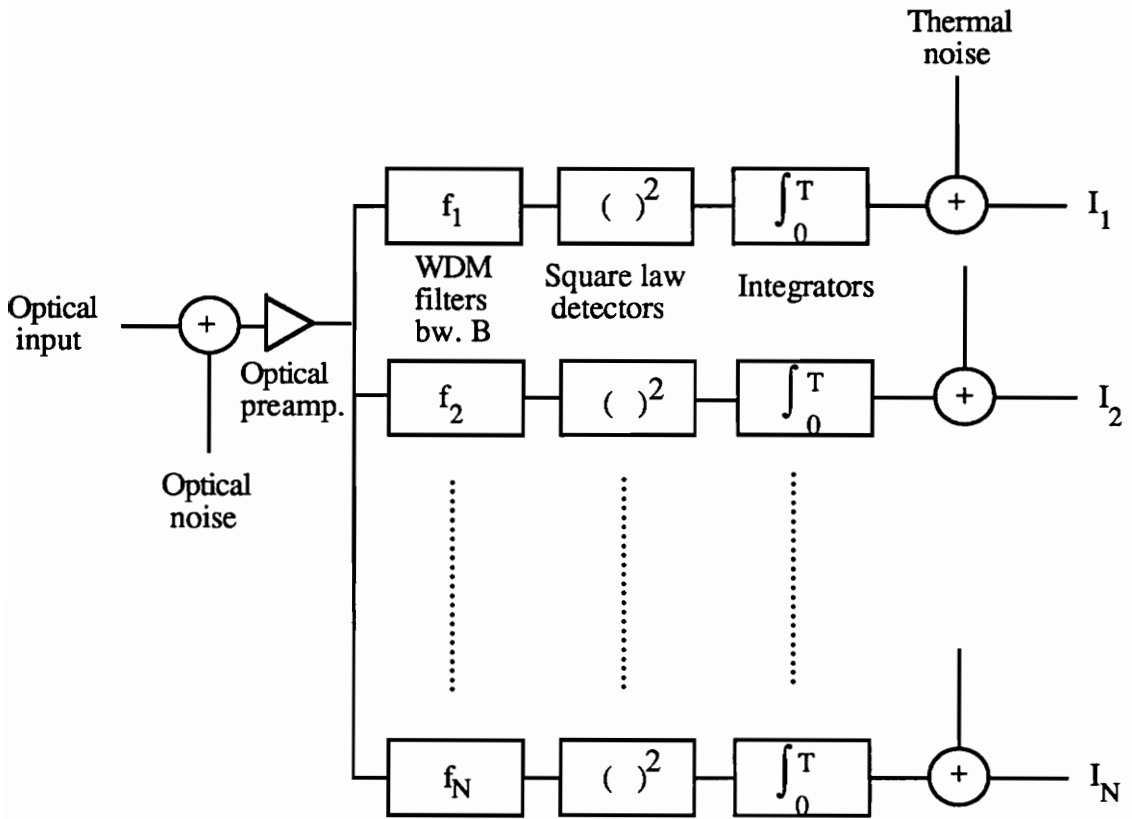


Figure 10. Receiver model for N-ary FSK system.

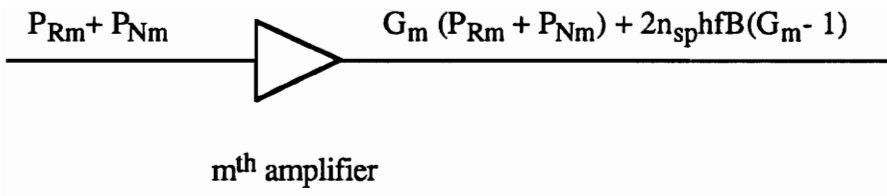


Figure 11. Optical amplifier model

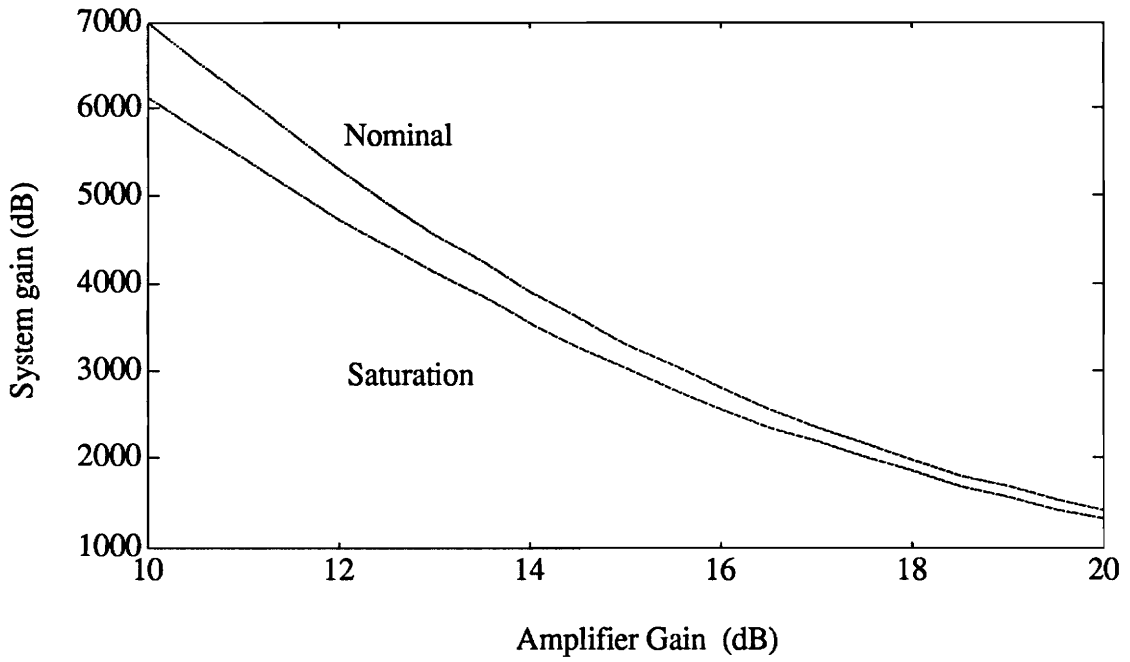


Figure 12. Effect of gain saturation in reducing maximum achievable system gain (Case I)
 $BT = 100$, $1/T = R_b = 2.5 \text{ Gb/s}$, $k = 7.95$, $P_T = 1 \text{ mW}$, $n_{sp} = 1.5$

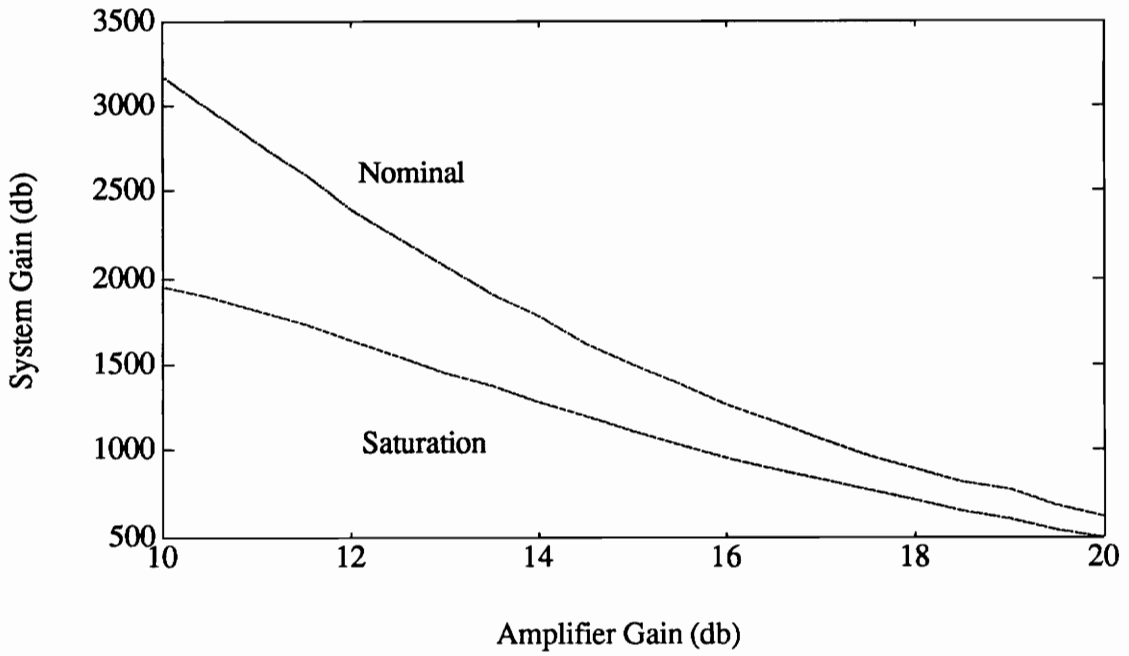


Figure 13. Effect of gain saturation in reducing maximum achievable system gain (Case I)
 $BT = 1000$, $1/T = R_b = 2.5 \text{ Gb/s}$, $k = 7.95$, $P_T = 1 \text{ mW}$, $n_{sp} = 1.5$

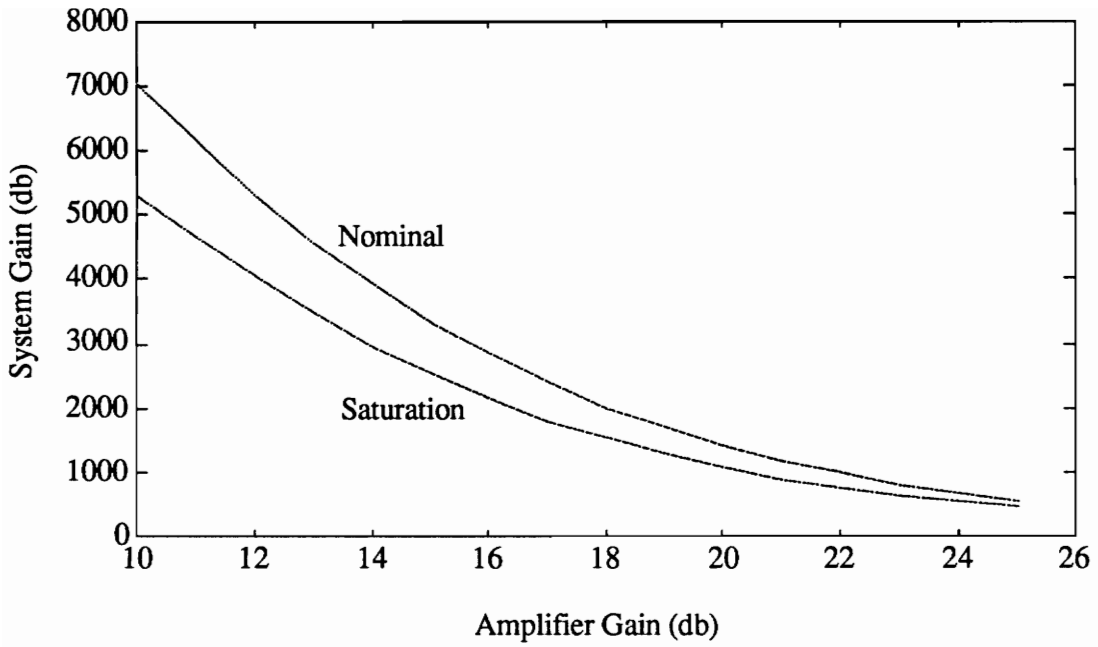


Figure 14. Effect of gain saturation in reducing maximum achievable system gain (Case II)
 $BT = 100$, $1/T = R_b = 2.5 \text{ Gb/s}$, $k = 7.95$, $P_T = 1 \text{ mW}$, $n_{sp} = 1.5$

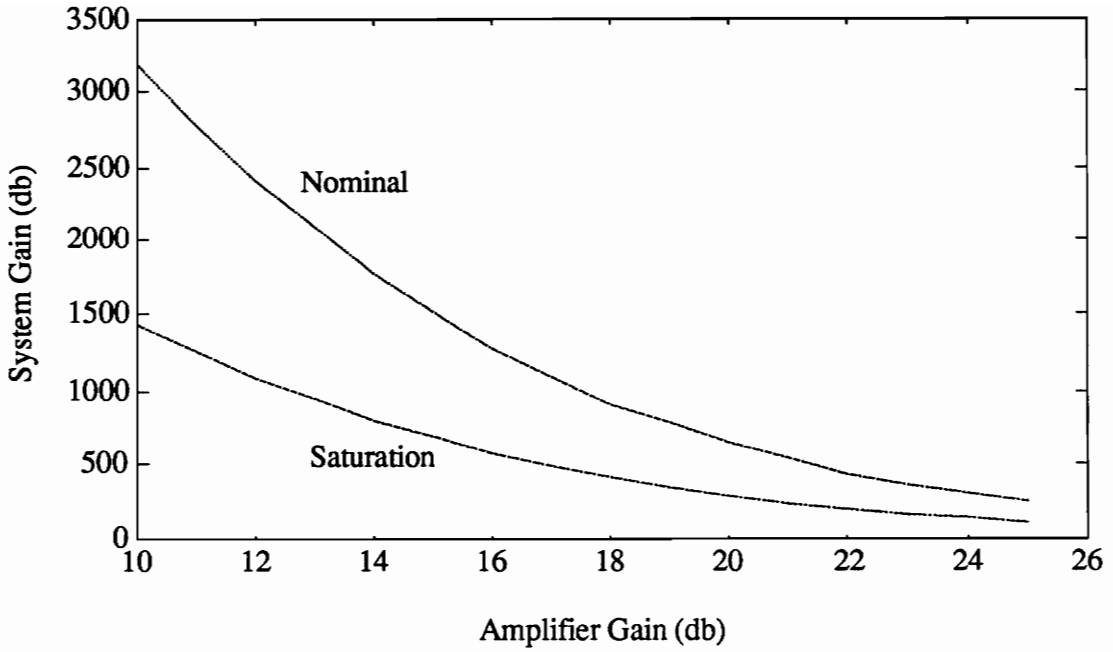


Figure 15. Effect of gain saturation in reducing maximum achievable system gain (Case II)
 $BT = 1000$, $1/T = R_b = 2.5 \text{ Gb/s}$, $k = 7.95$, $P_T = 1 \text{ mW}$, $n_{sp} = 1.5$

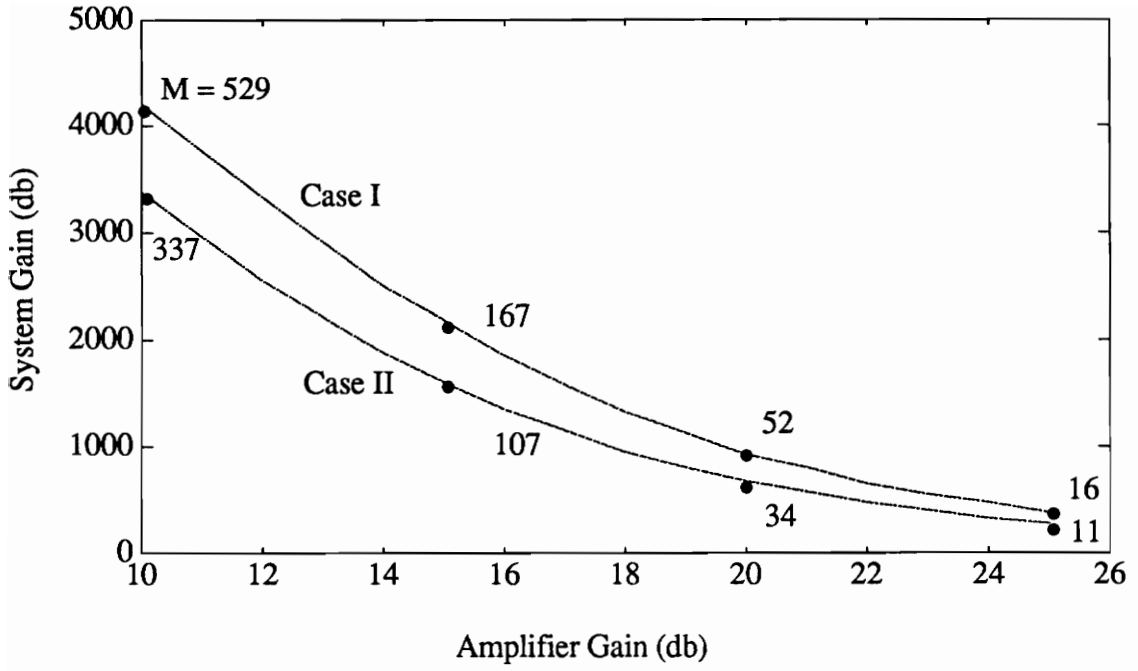


Figure 16. System Gain as a function of amplifier gain, for Cases I and II.
 $B = 5 \text{ nm}$, $1/T = R_b = 2.5 \text{ Gb/s}$, $k = 7.95$, $P_T = 1 \text{ mW}$, $n_{sp} = 1.5$

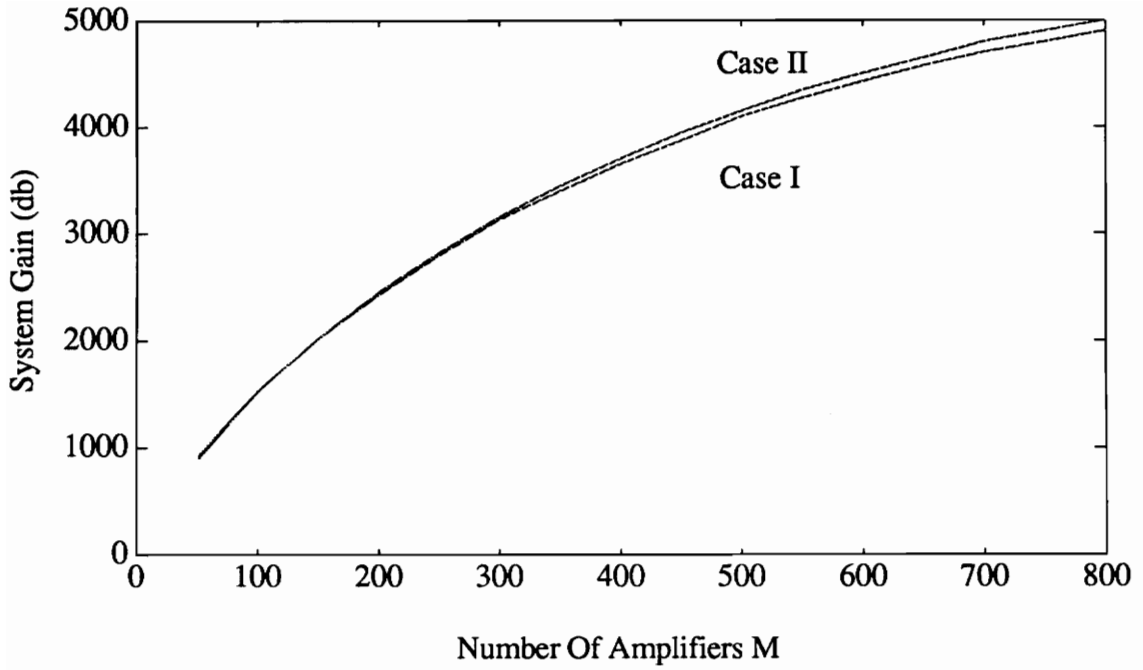


Figure 17. System Gain as a function of number of amplifiers used, for Cases I and II.
 $B = 5 \text{ nm}$, $1/T = R_b = 2.5 \text{ Gb/s}$, $k = 7.95$, $P_T = 1 \text{ mW}$, $n_{sp} = 1.5$

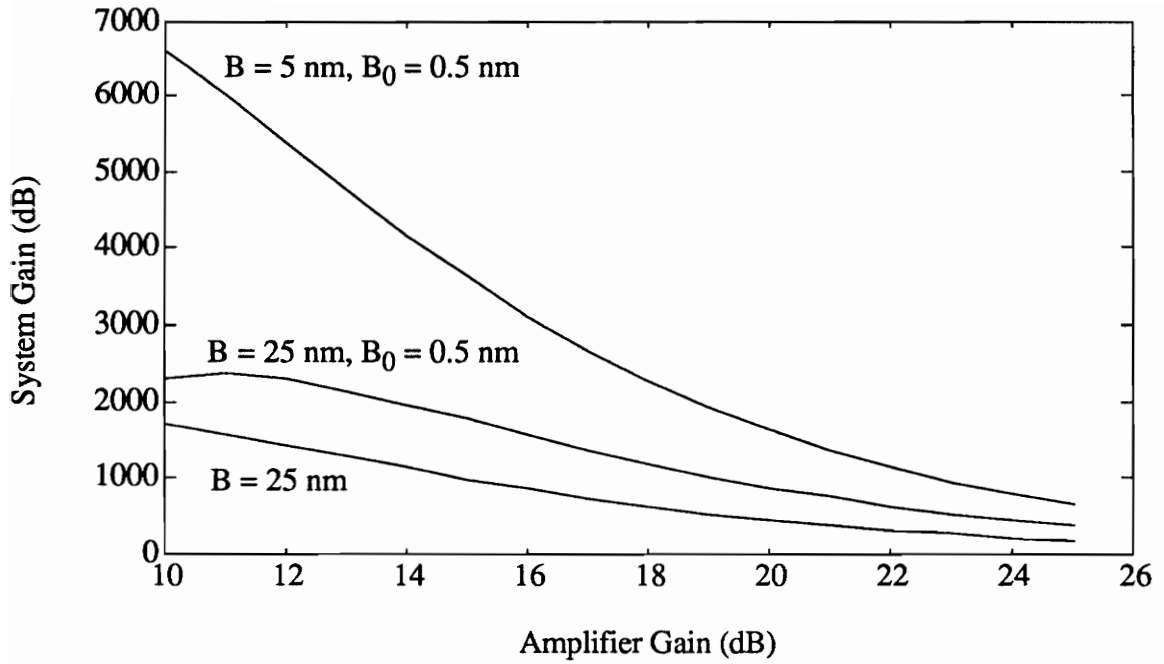


Figure 18. Effect of optical filtering on system gain for Case I.
 $1/T = R_b = 2.5 \text{ Gb/s}$, $k = 7.95$, $P_T = 1 \text{ mW}$, $n_{sp} = 1.5$

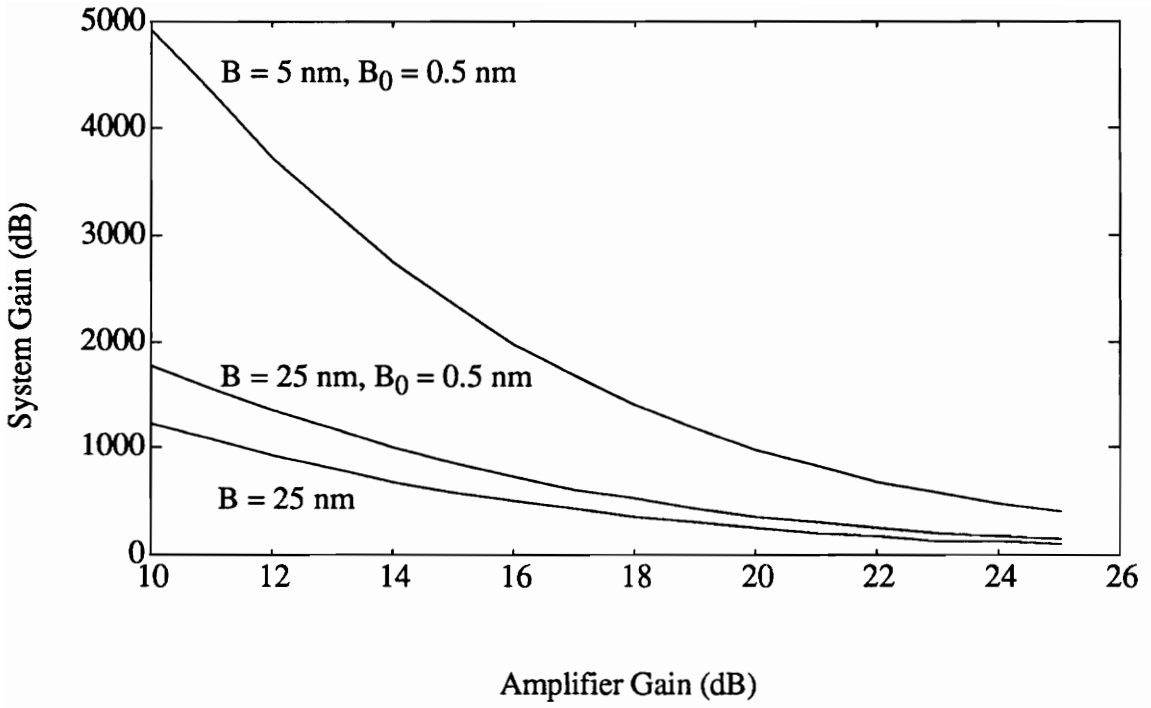


Figure 19. Effect of optical filtering on system gain for Case II.
 $1/T = R_b = 2.5 \text{ Gb/s}$, $k = 7.95$, $P_T = 1 \text{ mW}$, $n_{sp} = 1.5$

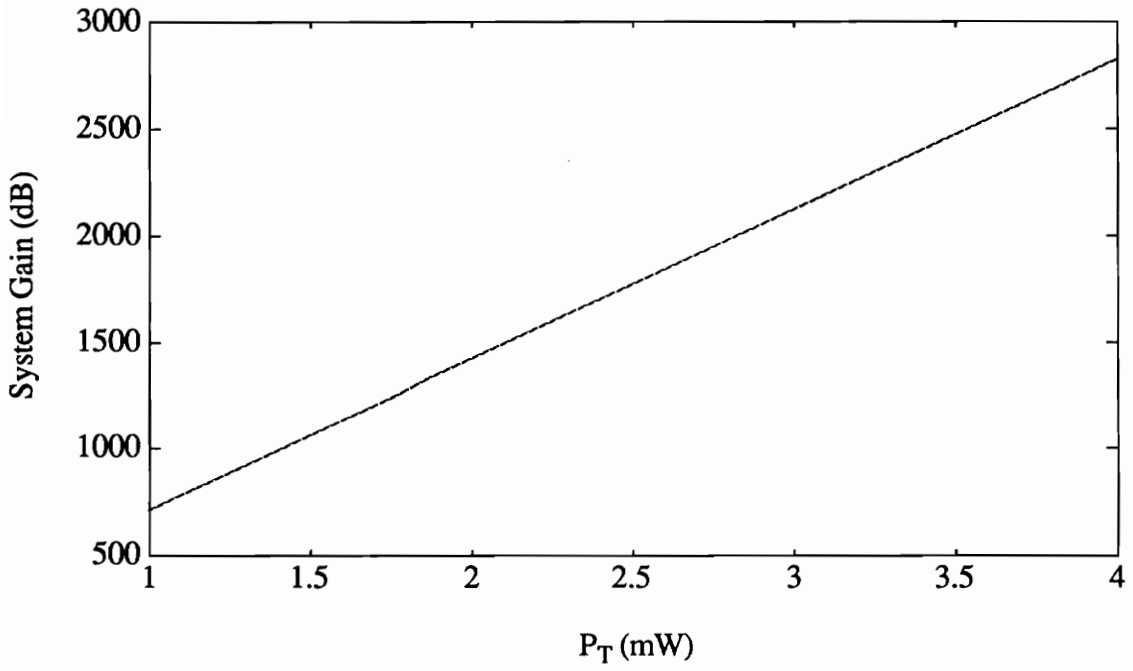


Figure 20. System gain as a function of transmitted power for Case II.
 $G = 20$ dB, $B = 5$ nm, $1/T = R_b = 2.5$ Gb/s, $k = 7.95$, $n_{sp} = 1.5$

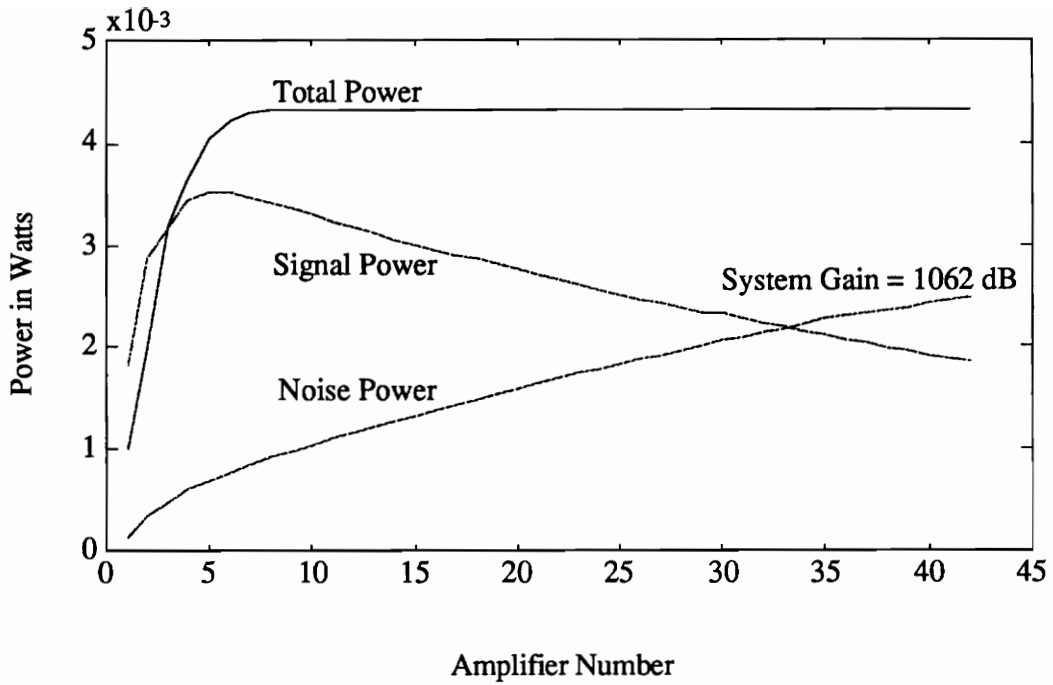


Figure 21. Propagation of signal and noise in a chain of identical, equally spaced amplifiers. G (unsaturated) = 30 dB, $G \cdot L = 3$, $B = 5$ nm, $1/T = R_b = 2.5$ Gb/s, $k = 7.95$, $P_{\text{sat}} = 4$ mW, $n_{\text{sp}} = 1.5$

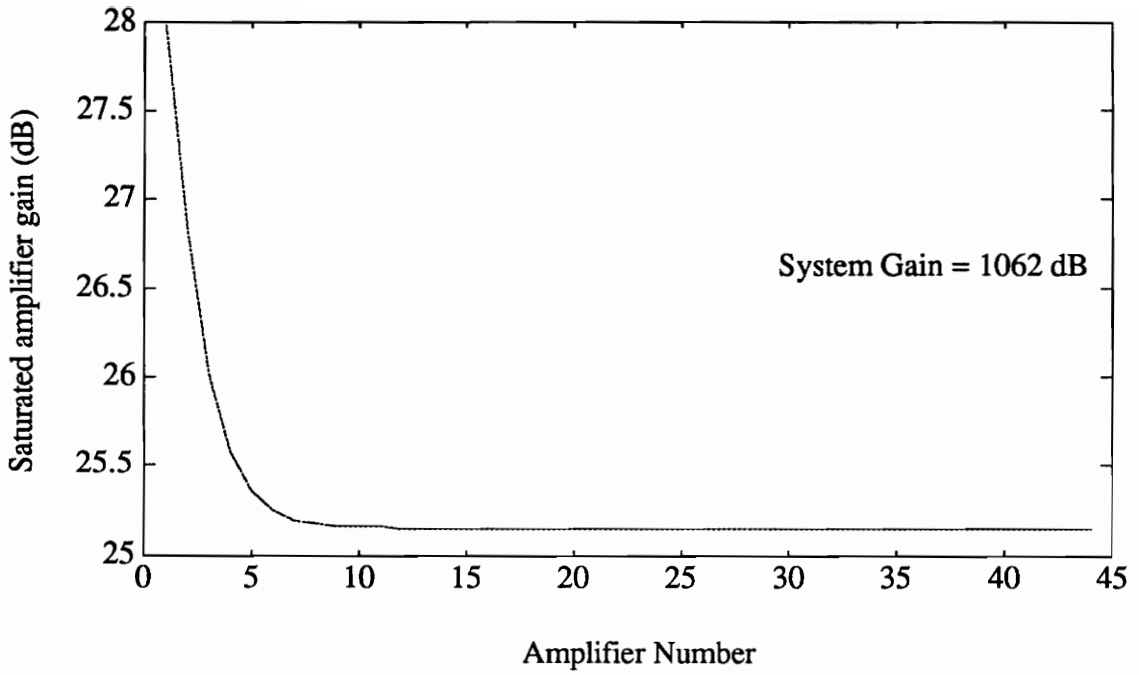


Figure 22. Saturated amplifier gains in a chain of identical, equally spaced amplifiers.
 G (unsaturated) = 30 dB, $G \cdot L = 3$, $B = 5$ nm, $1/T = R_b = 2.5$ Gb/s,
 $k = 7.95$, $P_{\text{sat}} = 4$ mW, $n_{\text{sp}} = 1.5$

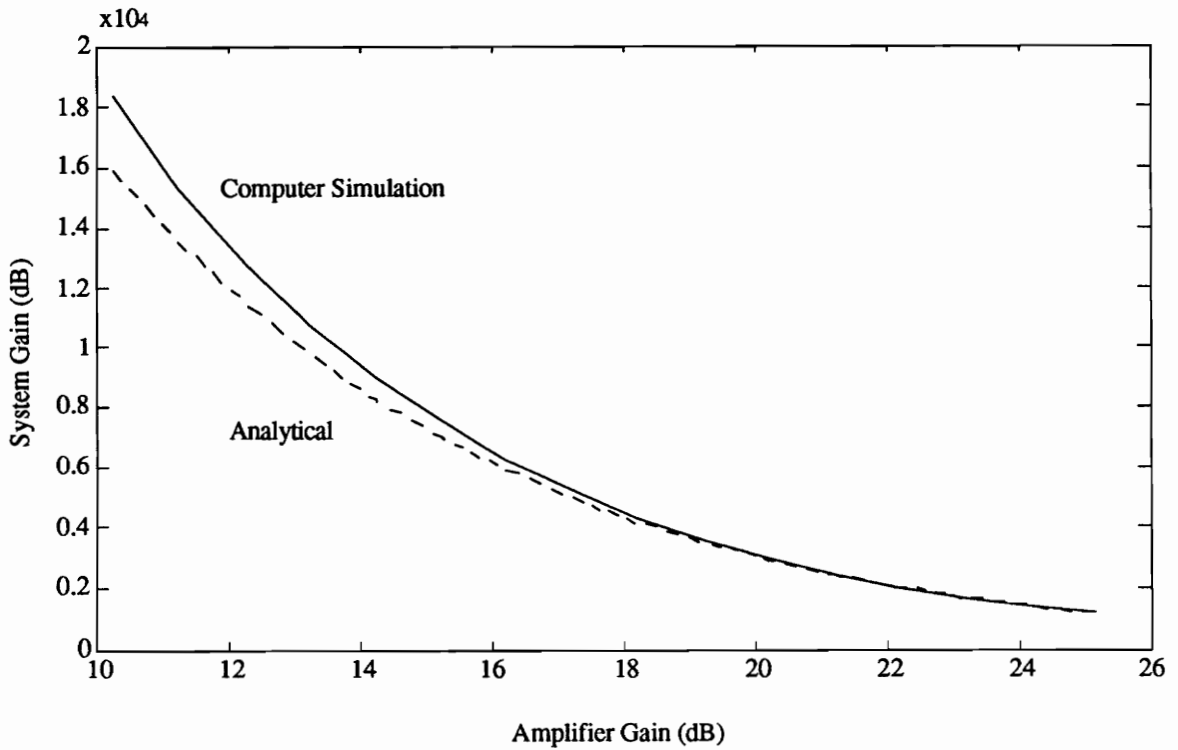


Figure 23. Comparison of system gain obtained by analytic formulae and by computer simulation.
 $G \cdot L = 3$, $B = 5 \text{ nm}$, $1/T = R_b = 2.5 \text{ Gb/s}$, $k = 7.95$, $P_{\text{sat}} = 4 \text{ mW}$,
 $n_{\text{sp}} = 1.5$

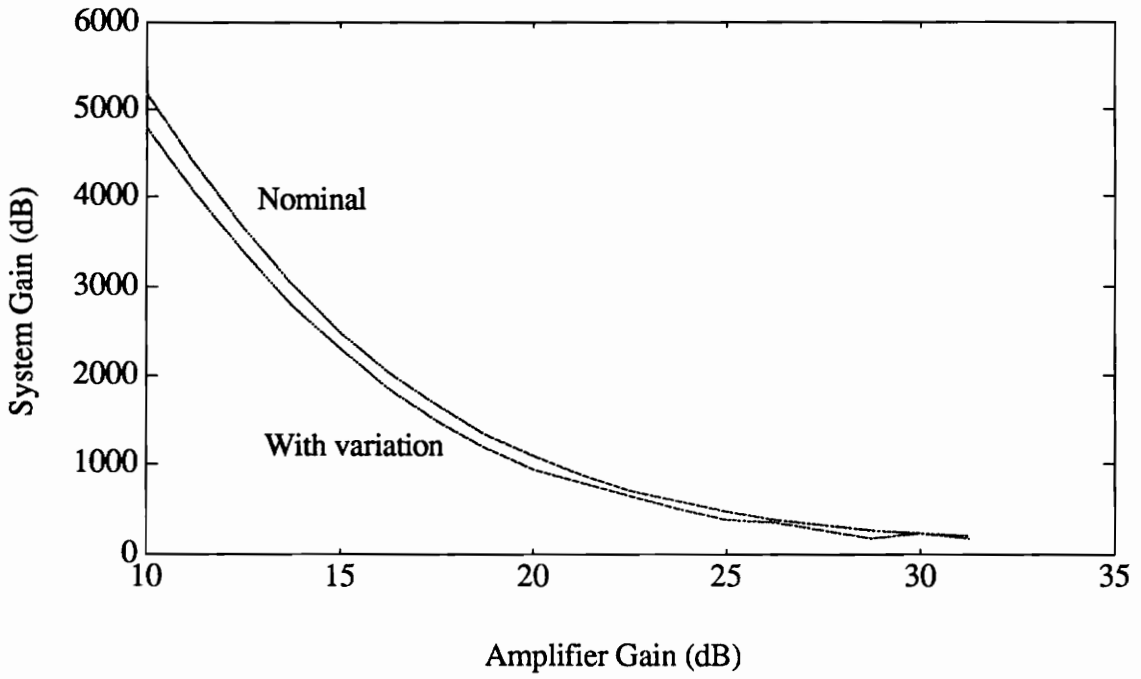


Figure 24. Effect of output power variations in reducing system gain.
 $1/T = R_b = 2.5 \text{ Gb/s}$, $k = 7.95$, $P_T = 1 \text{ mW}$, $n_{sp} = 1.5$, $B = 5 \text{ nm}$
 $B_0 = 0.5 \text{ nm}$, $\sigma = 0.26$ (1 dB power variation)

References

- [1] B. E. A. Saleh and M. C. Teich, *Fundamentals of Photonics*. New York : Wiley, 1990.
- [2] N. A. Olsson, "Lightwave Systems with Optical Amplifiers," *J. Lightwave Technol.*, vol.7, no. 7, pp. 1071-1082, July 1989.
- [3] I. Jacobs, "Effect of Optical Amplifier Bandwidth on Receiver Sensitivity," *IEEE Trans. on Commun.*, vol. 38, no. 10, pp. 1863-1864, October 1990.
- [4] P. A. Humblet and M. Azizoglu, "On the Bit Error Rate of Lightwave Systems with Optical Amplifiers," *J. Lightwave Technol.*, vol.9, no. 11, pp.1576-1582, November 1991.
- [5] C. R. Giles and E. Desurvire, "Propagation of Signal and Noise in Concatenated Erbium-Doped Fiber Optical Amplifiers," *J. Lightwave Technol.*, vol.9, no. 2, pp.147-154, February 1991.
- [6] I. Jacobs, "Communication Systems Implications of Optical Amplifiers," Internal Notes.
- [7] A. B. Carlson, *Communication Systems*. 3rd ed. New York : McGraw-Hill, 1986.

- [8] I. Jacobs and B. A. Raad, "Receiver Sensitivity of Lightwave Systems Using Optical Amplifiers," *Conf. Lasers and Electro-Optics (CLEO'91)*, Baltimore, MD, May 16, 1991.
- [9] D. Marcuse, "Derivation of Analytical Expressions for the Bit-Error Probability in Lightwave Systems with Optical Amplifiers," *J. Lightwave Technol.*, vol.8, no. 12, pp.1816-1823, December 1990.
- [10] P. S. Henry, "Error-Rate Performance of Optical Amplifiers," in *Opt. Fiber Commun. Conf. (OFC'89)*, Tech. Dig., ThK3, Houston, TX, February 9, 1989.
- [11] B. A. Raad, "Tunnel Filters and Optical Amplifiers for Use in Fiber Optic Communication Systems," *M.S. thesis*, VPI&SU, Blacksburg, VA, May 1991.
- [12] W. K. Pratt, *Laser Communication Systems*. New York : Wiley, 1969.
- [13] I. Jacobs, "The Asymptotic Behavior of Incoherent M-ary Communication Systems," *Proc. of the IEEE*, vol. 51, no. 1, January 1963.
- [14] J. G. Proakis, *Digital Communications*. New York : McGraw-Hill, 1983.
- [15] L. Eskildsen and E. Goldstein, "High-Performance Amplified Optical Links Without Isolators or Bandpass Filters," *IEEE Photon. Technol. Lett.*, vol. 4, no. 1, pp. 55-58, January 1992.

- [16] N. S. Bergano *et al.*, “ A 9,000 km 5 Gb/s and 21,000 2.4 Gb/s Feasibility Demonstration of Transoceanic EDFA Systems Using a Circulating Loop,” in *Proc. Opt. Fiber Commun. Conf. (OFC’91)*, San Diego, CA, PDP13, February 1991.
- [17] J. P. Blondel *et al.*, “Erbium-Doped Fiber Amplifier Spectral Behavior in Transoceanic Links,” in *Proc. Second Top. Meet. Opt. Amplifiers and Their Applications*, Snowmass, CO, ThA2, July 1991.
- [18] M. S. Pimpalkhare and I. Jacobs, “Maximum System Loss of Linearly Repeated Lightwave Systems,” submitted to *Third Top. Meet. Opt. Amplifiers and Their Applications*, June 1992.
- [19] A. E. Siegman, *Lasers*. Mill Valley, CA : University Science Books, 1986.
- [20] A. Papoulis, *Probability, Random Variables, and Stochastic Processes*. New York : McGraw-Hill, 1984.

Vita

Mangesh Shriniwas Pimpalkhare was born in Bombay, India on June 18, 1968. He received the B.Tech. degree in Electrical Engineering from the Indian Institute of Technology at Bombay, India in 1989. He was employed at the Fiber Optics Group in the department of physics at the Indian Institute of Technology at Delhi, India from 1989 to 1990. He graduated with an M.S. degree in Electrical Engineering from Virginia Polytechnic Institute and State University (Virginia Tech) in April, 1992. Since May, 1992 he has been employed with Intel Corporation, Folsom, CA. His research interests include fiber optics and semiconductor devices.

